



## Diversity and seasonal development of large zooplankton along physical gradients in the Arctic Barents Sea

Tom Van Engeland<sup>a,\*</sup>, Espen Bagøien<sup>a</sup>, Anette Wold<sup>b</sup>, Heather A. Cannaby<sup>a</sup>, Sanna Majaneva<sup>c</sup>, Anna Vader<sup>d</sup>, Jon Rønning<sup>a</sup>, Nils Olav Handegard<sup>a</sup>, Padmini Dalpadado<sup>a,\*</sup>, Randi B. Ingvaldsen<sup>a</sup>

<sup>a</sup> Institute of Marine Research (IMR), PO Box 1870, Nordnes, N-5817 Bergen, Norway

<sup>b</sup> Norwegian Polar Institute, Fram Center, Hjalmar Johansensgate 14, N-9007 Tromsø, Norway

<sup>c</sup> Department of Biology, Trondhjem Biological Station, Norwegian University of Science and Technology, NO-7491 Trondheim, Norway

<sup>d</sup> The University Centre in Svalbard (UNIS), PO Box 156, N-9171 Longyearbyen, Norway

### ARTICLE INFO

#### Keywords:

Arctic  
Northern Barents Sea  
Zooplankton  
Species composition  
Seasonality  
Environmental factors

### ABSTRACT

Due to ongoing climate change, a new Arctic Ocean ecosystem is emerging. Within the framework of the Nansen Legacy project, we investigated the community composition of the large zooplankton and its seasonal development along a latitudinal gradient in the northern Barents Sea. Total biomass was maximal in summer and early winter, and minimal in spring, with copepods contributing considerably in all seasons. Euphausiids represented a minor fraction of the biomass, whereas chaetognaths and other gelatinous zooplankton contributed substantially to the sampled zooplankton at all stations, particularly in winter. Amphipod biomass was high in early winter, but otherwise low. Temperature in the water column interior and bottom-depth had the highest explanatory power for the community composition of the large zooplankton, both revealing the same distinct Atlantic and Arctic domains along the studied section. The continental shelf of the northern Barents Sea had an Arctic signature and was in terms of biomass characterized by a dominance of cold-water species, such as *Themisto libellula*, and *Calanus glacialis*. The copepod *Calanus hyperboreus* was the dominant over the continental slope. Locations at the southern and northern end of the studied section were influenced by Atlantic Water (at intermediate depth at the northern stations), and contained a mixture of temperate species, deep-water species, and sympagic amphipods in northern ice-covered waters. In the northern Barents Sea, a seasonal change was observed in the biomass fractions of different zooplankton feeding guilds, with dominance of herbivores in summer and carnivores in winter. This suggests switching between bottom-up and top-down control through the year. On the continental slope, species that are typically considered omnivores seemed to increase in importance. The role of seasonally changing food preferences to bridge periods outside of the main primary production season is discussed in light of ecosystem resilience to the expected changes in the Arctic Ocean.

### 1. Introduction

Profound changes occur in the emerging new Arctic (Landrum and Holland, 2020), both in the biotic and abiotic environment. Diminishing of the sea ice due to warming and changes in the timing of the productive season is already happening in the Arctic Ocean (Dalpadado et al., 2020; Lewis et al., 2020). These changes may alter marine ecosystems, from phytoplankton to zooplankton to higher trophic levels (Arrigo and van Dijken, 2015). The northern Barents Sea is a focal point for some of these changes (Lind et al., 2018; Stroeve and Notz, 2018;

Brandt et al., 2023).

The internationally coordinated Nansen Legacy project was initiated in 2018 to investigate, among other goals, climate change impacts on high north marine ecosystems, and their biodiversity. The high Arctic waters are understudied, particularly with respect to large zooplankton due to challenges associated with sampling in ice covered waters. Studies from this region, covering a full seasonal cycle, are rare (but see for instance Basedow et al. (2018) for a seasonal study in the Fram Strait). The unprecedented warming, diminishing sea-ice, associated with Atlantification (Ingvaldsen et al., 2021) have made these high

\* Corresponding authors.

E-mail addresses: [tom.van.engeland@gmail.com](mailto:tom.van.engeland@gmail.com) (T. Van Engeland), [padmini.dalpadado@hi.no](mailto:padmini.dalpadado@hi.no) (P. Dalpadado).

<https://doi.org/10.1016/j.pocean.2023.103065>

Arctic waters more accessible in recent years. Our study provides baseline information on the community composition and seasonal development of large zooplankton from this rapidly changing area. The large zooplankton (copepods *Calanus glacialis* and *C. hyperboreus*, euphausiid *Thysanoessa inermis*, and amphipod *Themisto libellula*) are key prey of commercially and ecologically important fish species such as young North Atlantic cod, capelin, and polar cod in the region (Dolgov et al. 2011; Dalpadado and Mowbray 2013; Orlova et al. 2013; ICES, 2021).

The Barents Sea and the neighboring Eastern Fram Strait are inflow systems, where Atlantic Water is transported into the Arctic Ocean (Nansen, 1901). This Atlantic Water inflow is considered an important factor influencing the ecosystem dynamics of the region (Wassmann et al., 2020). Transport of warm Atlantic Water into the Barents Sea and the Arctic Ocean brings along Atlantic species which alter the local zooplankton community composition directly (Dalpadado et al., 2012; Basedow et al., 2018). Hence, species composition may correlate with water mass characteristics. Gluchowska et al. (2017) observed increasing contributions of Atlantic copepod species to the Fram Strait zooplankton communities, linked to positive temperature anomalies caused by the Atlantic Water (AW) transport. Similarly, Mañiko et al. (2020) found distinct water mass signatures in the diversity of gelatinous zooplankton in early summer in the Fram Strait. Water mass characteristics and water depth were also found to be associated with the mesozooplankton community composition north of Svalbard during

the first part of the productive season (Hop et al., 2021). These studies indicate the importance of boreal organisms carried into the Arctic by Atlantic water inflows, impacting local Arctic species diversity.

Besides the direct transport of zooplankton, heat transport changes the environmental conditions, making them less or more permissive for species at the edge of their tolerance window. Northern euphausiid species are mostly restricted to the boreal/Atlantic Water of the Barents Sea (Dalpadado et al., 2008a). But as a consequence of the Atlantification of the Arctic, the euphausiid distribution has expanded northwards in recent decades (ICES, 2020). Sympagic fauna and organisms associated with the ice edge, on the other hand, are lost from the local surface community as a result of sea ice retreat under increased heat input (Søreide et al., 2010; David et al., 2015; Ehrlich et al., 2020; Ershova et al., 2021). Flores et al. (2019) found that the taxonomic composition of the under-ice fauna in the Eurasian sector of the Arctic was mainly driven by water mass characteristics and sea ice properties, whereas the trophic community structure was more associated with variation in nutrients. These examples show that the abiotic environment to a considerable extent shapes zooplankton diversity and distribution in the Arctic.

Besides these bottom-up effects, temperature, light, and a shift from perennial to seasonal ice or open water will enable visual predators to extend their feeding range (Langbehn and Varpe, 2017), thus increasing top-down effects on the zooplankton community (Orlova et al., 2013; Kaartvedt and Titelman, 2018).

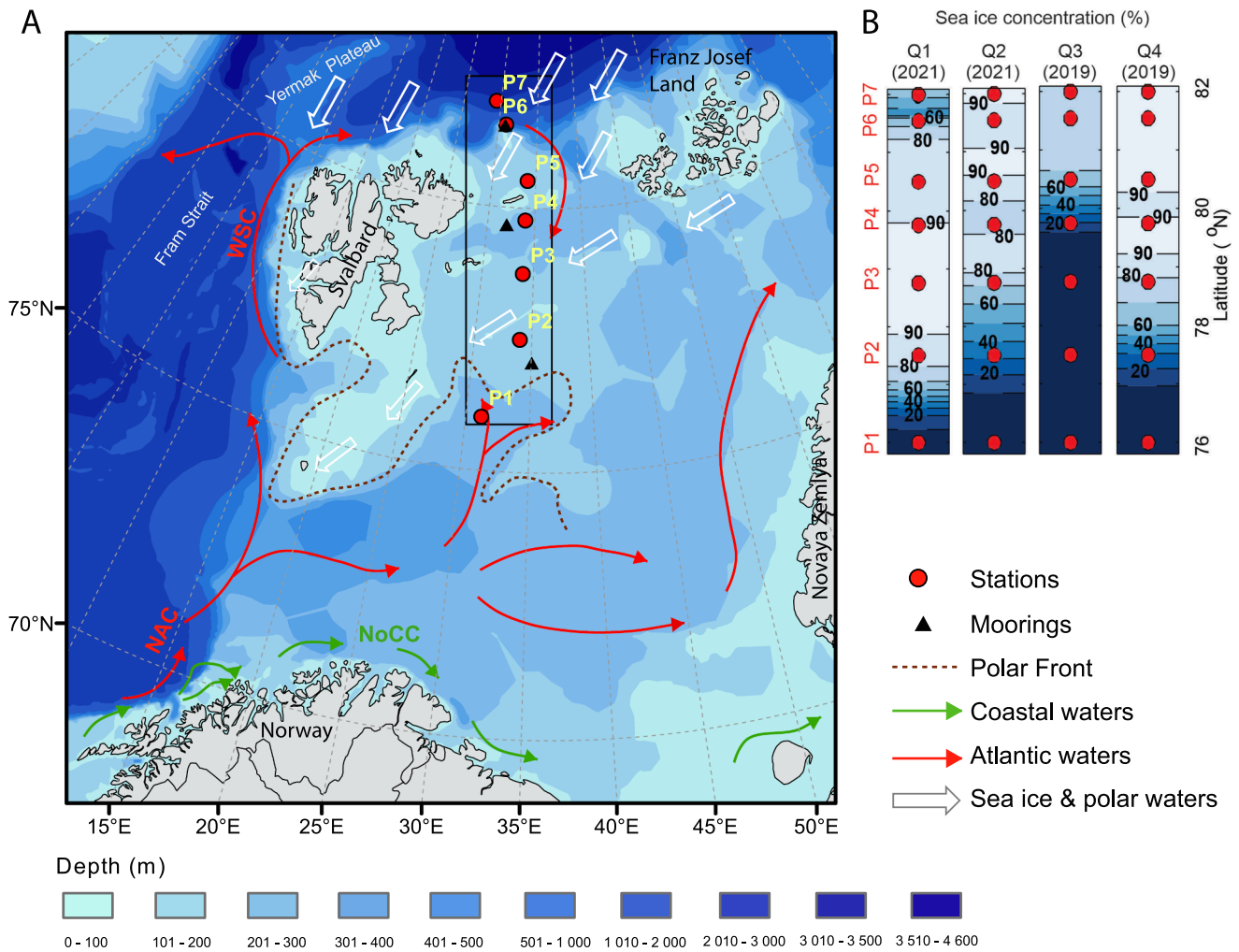


**Fig. 1.** Position of the sampling stations (red dots) and mooring stations (black triangles) in the northern Barents Sea (A). The current systems NAC (Norwegian Atlantic Current), NoCC (Norwegian Coastal Current), and WSC (West-Spitsbergen Current) are indicated in the colors of their respective water masses. Sea ice concentration (%) along the south-to-north section (B) during the seasonal surveys in 2019 and 2021. The sea ice concentration values are also given in Table 1.

In the context of the Nansen Legacy project, four surveys were conducted, spanning the entire gradient of the Marginal Ice Zone, from the central Barents Sea into the Arctic Ocean. These surveys covered a full seasonal cycle (Fig. 1), including the Arctic winter for which data is sparse. On each of these surveys the community of the large zooplankton was systematically sampled at seven locations, allowing for a seasonal study of the diversity and spatio-temporal distribution of the key species. The objective of this paper is to investigate the role of physical (sea ice cover, temperature, and bottom depth) and biological (chlorophyll *a* concentration) factors in shaping the overall community composition of the large zooplankton in this region of the Arctic. Our hypothesis is that the spatial variability of the community composition of the large zooplankton is governed by the water mass characteristics along the investigated latitudinal gradient. In addition, we report on the regional composition of the large zooplankton in winter, a season that is under-represented in Arctic research.

## 2. Materials & methods

### 2.1. Site description

The transport of Atlantic Water into the Barents Sea can be roughly subdivided into: 1) a relatively narrow and fast northward flowing branch through the Fram Strait, the West-Spitsbergen Current (WSC), that turns eastward in the vicinity of the Yermak Plateau (Crews et al., 2019), and 2) a wider and slower eastward flowing branch, that flows over the continental shelf of the Barents Sea and enters the Arctic Ocean east of Franz Josef Land (Rudels et al., 2015). Part of the Atlantic Water flow crossing the Yermak plateau also enters the northern Barents Sea from the north (Lind and Ingvaldsen, 2012).

The Polar Front separates the warm Atlantic Water in the southern Barents Sea from colder and more Arctic conditions in the north (Fig. 1). Thus, the Barents Sea has two climatic domains where the southern one is strongly influenced by the inflow of warm Atlantic Water (Loeng, 1991), while the northern (Arctic) one is dominated by sea ice and polar waters maintaining a strong ocean stratification (Lind et al., 2018).

### 2.2. Surveys and sampling design

As part of the Nansen Legacy project, four surveys with the ice breaker R/V *Kronprins Haakon* were organized covering four seasons (quarters; Q1-Q4). Due to the Coronavirus pandemic, the summer and early winter surveys (Q3 and Q4) were performed in August and December 2019, whereas those from late winter and spring (Q1 and Q2) had to be postponed until March and May 2021, respectively. A south-to-north section with 7 stations (P1-P7) was sampled on each of these surveys, covering latitudes from the central Barents Sea (P1) to just north of the continental slope (P7), with the typical topography of banks and troughs (Fig. 1, Table 1).

Samples of the macrozooplankton and large copepods (hereafter collectively called large zooplankton) were collected by hauls with a Midwater Ring Net (commonly referred to as MIK net) with 3.14 m<sup>2</sup>

aperture, ~13 m length, with a ~ 1600 μm mesh size except for the last 1 m having 500 μm (ICES, 2017). The MIK was fitted with a 10-liter cod-end and a flow meter mounted at the entrance of the net.

One sample was collected at each of the seven aforementioned stations along the section in four different seasons Q1 (March), Q2 (May), Q3 (August) and Q4 (December; Fig. 1, Table 1), resulting in a total of 28 samples. On all surveys, vertical hauls were made, except in the very first survey (Q3), where oblique hauls were taken at the open water stations P1, P2, and P3, aiming for a net speed of ca. 1.75 m s<sup>-1</sup>. As it was not possible to make oblique hauls in the ice-covered waters, it was decided to operate with vertical hauls as the standard routine at the remaining stations and on the subsequent surveys. Samples were collected from ~ 20 m above the bottom to the surface, except at the deeper station P7 (Table 1). A hauling speed of ca. 1.5 m s<sup>-1</sup> was used. Due to the open-net-to-inlet-area ratio, potential bucket effects (water pushed away in front of the opening at high hauling speeds) are considered negligible at the operating speed used in this study (ICES, 2017).

### 2.3. Sample processing and storage

The gelatinous zooplankton species captured in the MIK net were sorted out immediately after collection, as they are subject to quick degradation. They were gently removed using filtering spoons or wide-mouthed pipettes and kept in seawater in the refrigerator until identified to the highest taxonomic level possible. In addition, the total number of individuals was recorded. Some individuals of each taxon (up to 12 individuals) were length measured and photographed using a lightboard including millimeter reference. Subsequently, they were weighed and stored individually with > 96% non-denatured EtOH and kept at -20 °C for later genetic confirmation. Biomasses of *Aglantha digitale* and *Beroe* sp. at station P1, *Beroe* sp. at P3, *Mertensia ovum* at P4, and *Aglantha digitale* at P5 in the May survey (Q2) should be regarded as minimum estimates due to uncertainties in handling onboard. The gelatinous zooplankton sample from station P7 during the Q4 survey was lost.

After the removal of the gelatinous zooplankton, other zooplankton taxa that were only found in low numbers were isolated, weighed and stored in zip-lock bags in the freezer at -20 °C. Finally, a quantitative weighed portion of the remainder of the MIK catch was stored in hexamine-buffered 4% formalin for detailed taxonomic analyses at the IMR laboratory. Smaller samples were processed in total, while sub-samples were taken in larger ones using a Motoda splitter. In the laboratory, the zooplankton from the formalin and frozen samples was sorted, identified to group/species level, counted, weighed, and length-measured individually. The length measurements were conducted only on randomly selected samples of euphausiids and amphipods.

Note that the preservation of biological material in formalin implies that the wet weight may change slightly relative to the initial wet weight after sampling. Only the larger-sized copepods (mostly copepodite stage V and adults) were included in our analyses as the smaller individuals (younger copepodite stages and smaller species) were not quantitatively sampled by the MIK net. Furthermore, the possible net avoidance

**Table 1**

Overview of stations with the sampling depth and ice concentration in the four sampled seasons, with an indication of the month of sampling.

Station	Latitude (°N)	Longitude (°E)	Water depth (m)	Sampling depth (m)	Sea ice concentration (%)			
					Q1 (Mar 2021)	Q2 (May 2021)	Q3 (Aug 2019)	Q4 (Dec 2019)
P1	76.00	31.22	322	312	0	0	0	1
P2	77.50	34.00	190	180	86	32	0	28
P3	78.75	34.00	301	291	94	71	0	77
P4	79.75	34.00	332	322	91	77	19	92
P5	80.50	34.00	167	157	84	90	67	92
P6	81.55	30.85	865	855	67	87	75	92
P7	82.00	30.00	3000	1000 *	63	92	73	94

\* Note that for station P7 the lower sampling-depth was 2000 m on cruise Q3 (Aug 2019) while 1000 m on all other cruises.

behavior of larger organisms such as krill and amphipods that might swim away from the path of the approaching net implies that the MIK catches represent relative rather than absolute *in situ* abundance and biomass (Dalpadado et al., 2016). The zooplankton data is accessible here: <https://doi.org/10.21335/NMDC-1549427017>.

#### 2.4. CTD and additional data collection

A shipboard conductivity, temperature, and depth profiler (Seabird 911plus CTD), attached to a 24-bottle rosette system was deployed on 24 locations along the section, including our 7 sampling stations during each season. From the sampled water, chlorophyll *a* (Chl *a*) concentrations ( $\text{mg m}^{-3}$ ) were spectrophotometrically determined at various depths. These data are published at the Norwegian Marine Data Centre (Vader, 2022). The values of the upper 50 m of the water column were averaged per station.

Sea ice concentration (SIC) during the surveys was calculated based on daily sea ice concentrations from Nimbus-7 SMMR and DMSP SSM/I-SSMIS Passive Microwave Data received from NSIDC (Cavalieri et al., 1996).

To assess the timing of the surveys regarding the seasonal cycle, we needed continuous sea surface temperature (SST) measurements at stations P1-P7, covering the entire study period. These were extracted from the OSTIA global foundation Sea Surface Temperature product (Good et al., 2020, obtained from the E.U. Copernicus Marine Service Information website; <https://doi.org/10.48670/moi-00165>). SST in ice-covered waters was set to the freezing temperature (approximately  $-1.8^\circ\text{C}$ ).

To assess the impact of non-consecutive sampling seasons, we explored seasonal and annual variability in SIC, SST, and temperature time series from three Nansen Legacy moorings over the period 2019–2021 (Fig. 1). Mooring M5-Bio was located near P2 (at  $77.1^\circ\text{N}$ ,  $35.1^\circ\text{E}$ ) and had a Nortek Signature 100 Acoustic Doppler Current Profiler (ADCP) located at 136 m depth (during 11.08.2019–28.09.2020) and 140 m depth (during 13.10.2020–07.11.2021). Mooring M2 was deployed near P4 ( $79.7^\circ\text{N}$ ,  $32.3^\circ\text{E}$ ). For this study we used data from a RBR Concerto deployed at 210 m depth (before 17.11.2019), at 220 m depth (during 18.11.2019–23.09.2020) and at 185 m depth for the remainder of the time series (Lundesgaard et al., 2022). Mooring ATWAIN-BioAC was located near P6 (at  $81.5^\circ\text{N}$ ,  $30.8^\circ\text{E}$ ) and had a Nortek Signature 100 ADCP located at 400 m depth (during 23.11.2019–04.09.2020) and 453 m depth (during 30.09.2020–14.09.2021).

Feeding guilds were assigned at the species or genus level based on the literature (Table S1). A distinction was made between 1) carnivores, 2) omnivores, and 3) herbivores and detritivores combined. When different papers mentioned a carnivorous and omnivorous feeding strategy for a particular species, for instance as part of their seasonality, it was assigned to the omnivore feeding guild.

#### 2.5. Data processing and statistical analyses

##### 2.5.1. Biotic data

The total masses were divided by the filtration volumes per sampling event, to obtain biomass concentrations in terms of wet weight ( $\text{g wet wt. m}^{-3}$ ). Filtration volumes (*V*) were calculated as:

$$V = A \times d,$$

where *A* is the MIK's mouth opening area ( $3.14 \text{ m}^2$ ), and *d* is the distance traveled by the MIK during the haul. This distance was for oblique hauls calculated as:

$$d = \text{flow meter revolution counts} \times 0.3,$$

where 0.3 is the HYDRO-BIOS multiplication factor (i.e. propeller pitch; cf. equipment manual, Hydro-BIOS GmbH). For vertical hauls, the

maximal wire length was assumed as the traveled distance (*d* = wire length), because flow meter readings were not available for all vertical hauls. The biomass integrated over the water column ( $\text{g wet wt. m}^{-2}$ ) was calculated as the biomass concentrations multiplied by the sampling depth (Table 1).

##### 2.5.2. CTD data

CTD signals from above 15 m depth were discarded to avoid contamination of the signals by ship movement and the proximity of the ship's moon pool from which the CTD was lowered. For inclusion in the multivariate analyses (see next section), average values of temperature (*T*), salinity (*S*) and potential density ( $\sigma_\theta$ ) were calculated for two layers in the water column (Table S2). For the upper water column, mean values were calculated over the depth range of 15–25 m (indicated by a subscript 20 m, e.g.  $T_{20\text{m}}$ ). This depth was chosen because it was above the summer pycnocline. For the water column interior, average values were calculated for the depth range 145–155 m (indicated by a subscript 150 m, e.g.  $T_{150\text{m}}$ ), because this was always below the pycnocline when it was present.

CTD data were categorized into water masses using a minor adjustment of the water mass definitions outlined for the Nansen Legacy project (Sundfjord et al., 2020). This includes the relatively warm and saline Atlantic Water (AW) and the slightly colder modified Atlantic Water (mAW). Using the characteristics  $T > 0.0^\circ\text{C}$ ,  $S \geq 34.89$  include both (AW/mAW). Polar Water (PW) is cold and fresh and identified by  $T \leq 0.0^\circ\text{C}$ ,  $\sigma_\theta \leq 27.97 \text{ kg m}^{-3}$ , and this water mass is common in the Arctic domain north of the Polar Front (Fig. 1). PW that has been heated through solar radiation or mixing with AW/mAW is called Warm Polar Water (wPW), and is characterized by  $T > 0.0^\circ\text{C}$ ,  $S < 34.89$  psu (Sundfjord et al., 2020). PW includes waters that historically were defined as Arctic Water in the Barents Sea (Loeng, 1991), but the PW definition includes slightly more saline waters than usually included in the Arctic Water definition. The reason for using PW and wPW instead of Arctic Water is to bridge water mass definitions in the northern Barents Sea with those commonly used in the Nansen Basin (Sundfjord et al., 2020). Cold water masses found deeper in the water column include Intermediate Water (IW characterized with  $-1.1^\circ\text{C} < T \leq 0.0^\circ\text{C}$ ,  $\sigma_\theta > 27.97 \text{ kg m}^{-3}$ ) and the coldest and densest water mass called Cold Barents Sea Deep Water (CBSDW, characterized by  $T \leq -1.1^\circ\text{C}$ ,  $\sigma_\theta > 27.97 \text{ kg m}^{-3}$ ). These water masses were used as environmental variables in statistical analyses of diversity indices (cf. Section 3.5).

##### 2.5.3. Statistical analyses

All statistical analyses and data processing were performed in the R Statistical Software (R Core Team, 2020). Statistical testing of seasonal and spatial effects on biomass of large zooplankton, as well as relationships between biomass and environmental variables, was performed by generalized linear modeling (linear regression, analysis of variance = ANOVA, and analysis of covariance = ANCOVA) using the 'nlme' R-package (Pinheiro et al., 2020). When required, log-transformations of the independent and/or dependent variables were performed to obtain symmetric distributions. The sea ice concentration (SIC) in these analyses was transformed to the percentage of open water (%OW; Table S2) as:

$$\%OW = 100 - SIC.$$

To characterize the diversity of the large zooplankton along the section and over the seasons, Shannon-Weaver diversity (*H*), taxon richness (*S*), and Pielou's evenness (*J*) were calculated using the R-package 'vegan' (Oksanen et al., 2019). These indices are defined as follows (Legendre and Legendre, 2012):

*S* = number of taxa in the sample,

$$H = - \sum_{i=1}^S p_i \log_e p_i$$

$$J = \frac{H}{\log_e(S)}$$

where  $p_i$  is the proportion of species  $i$  in the sample (on a biomass basis, not abundance). These indices were calculated at the highest available taxonomic level. Effects of environmental variables on these indices

were tested using simple linear models.

Canonical Correspondence Analysis (CCA) was used to investigate relationships between the taxonomic composition of large zooplankton (including *Calanus hyperboreus* and *C. glacialis*, but excluding other copepod species) and environmental variables (Greenacre, 1983, 2017; Legendre and Legendre, 2012; Greenacre and Primicerio, 2013). CCA is

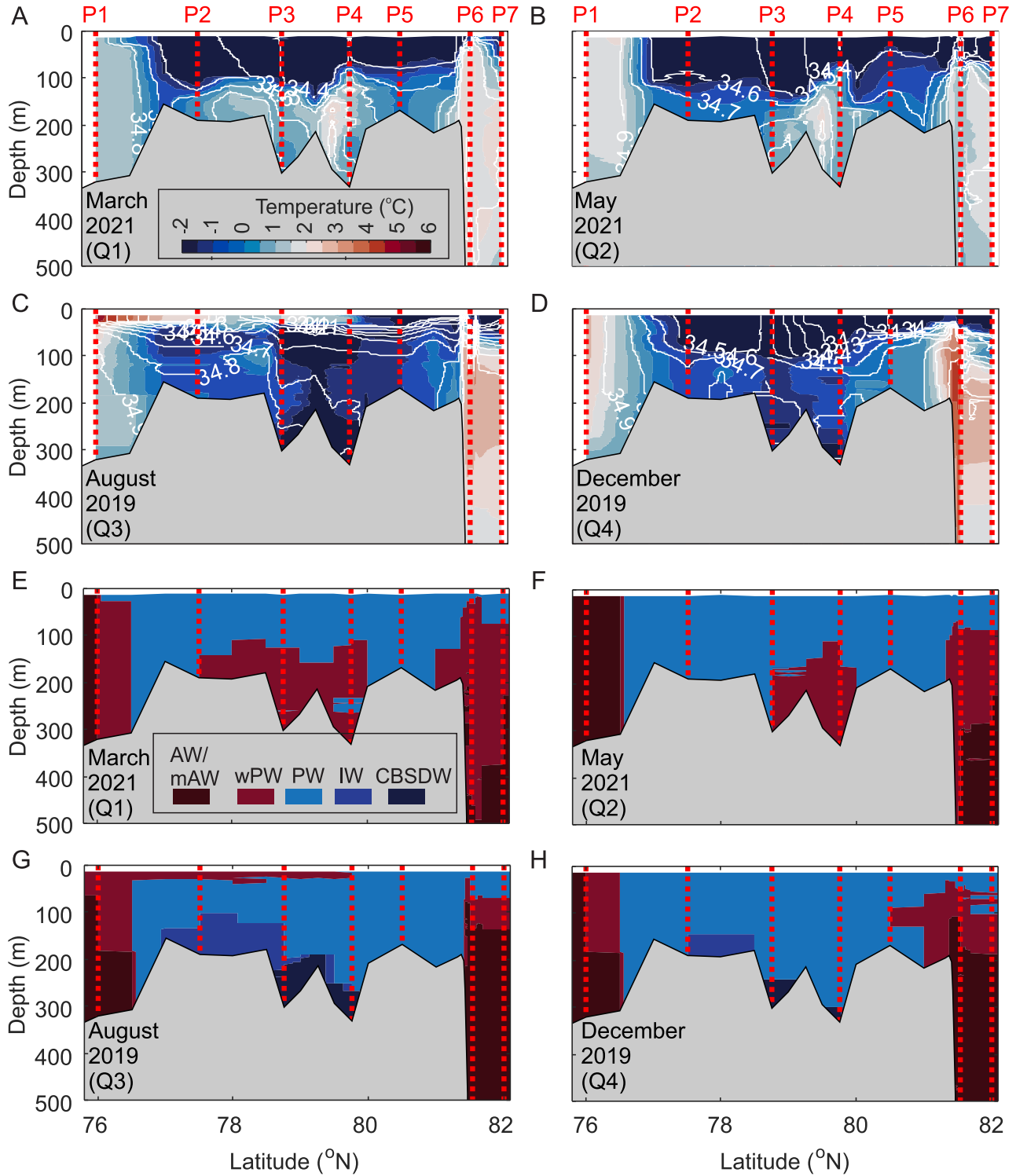


**Fig. 2.** Water column temperature (color) and salinity (contour) during the 4 seasonal surveys (A-D) and the associated water mass distributions (E-H; AW = Atlantic Water, mAW = modified Atlantic Water, PW = Polar Water, wPW = warm Polar Water, IW = Intermediate Water, CBSDW = Cold Barents Sea Deep Water). Water masses with a temperature above 0 °C are shown in dark red while water masses with sub-zero temperatures are shown in blue. Sampling stations for the large zooplankton are indicated as red dashed lines.

a constrained multivariate gradient analysis, where the response data (in our case biomass concentrations of various large zooplankton taxa) are related to the predictor variables (environmental data; cf. Table S2 in the Electronic supplement). CCA was performed using the R-package ‘vegan’ (Oksanen et al., 2019). The biomass concentrations were double square-root transformed. The highest available taxonomic resolution was consistently used throughout all stations and seasons (species level for the most common taxa, genus level for less common taxa). Taxa with only one observation (7 taxa) were excluded from the analysis to avoid a disproportionate influence on the final result. A forward stepping procedure was used to select informative combinations of significant environmental variables. This selection was done by first including the variable with the highest explanatory power, thereafter, adding other variables with significant marginal effect one at the time, while taking care not to introduce excessive collinearity ( $Pearson's\ r^2 < 0.25$  between included environmental variables; cf. Fig. S4 in the Electronic Supplement; ter Braak and Verdonschot, 1995). The testing of significance was performed using 20,000 permutations. In the CCA analysis, all taxa for station P7 at cruise Q4 (Dec 2019) were excluded due to missing data for gelatinous plankton. To check the robustness of our results, we repeated

the CCA including P7 at cruise Q4 but excluding gelatinous plankton from all stations. Grouping of stations in the CCA plots was based on visual inspection of the plot, and ellipses were drawn with the ‘ordiellipse’-function from the ‘vegan’ R-package.

### 3. Results

#### 3.1. Spatio-temporal variability in hydrography

Strong differences in temperature and salinity were found among the stations (Fig. 2). The southernmost (P1) and northernmost (P6 and P7) stations were characterized by relatively warm ( $T > 0\text{ }^{\circ}\text{C}$ ) and saline AW/mAW or wPW. The continental slope stations, P6 and P7, resembled station P1 with respect to the water below the pycnocline, and the warm core of AW was year-round detectable on the continental slope below 100 m depth. The stations at the northern Barents Sea shelf (P2-P5) on the other hand, were generally dominated by colder ( $T < 0\text{ }^{\circ}\text{C}$ ) and fresher water masses and stronger vertical stratification (mostly due to salinity). The temporal variation was largest near the surface, revealing substantially warmer and fresher (and more stratified) conditions during

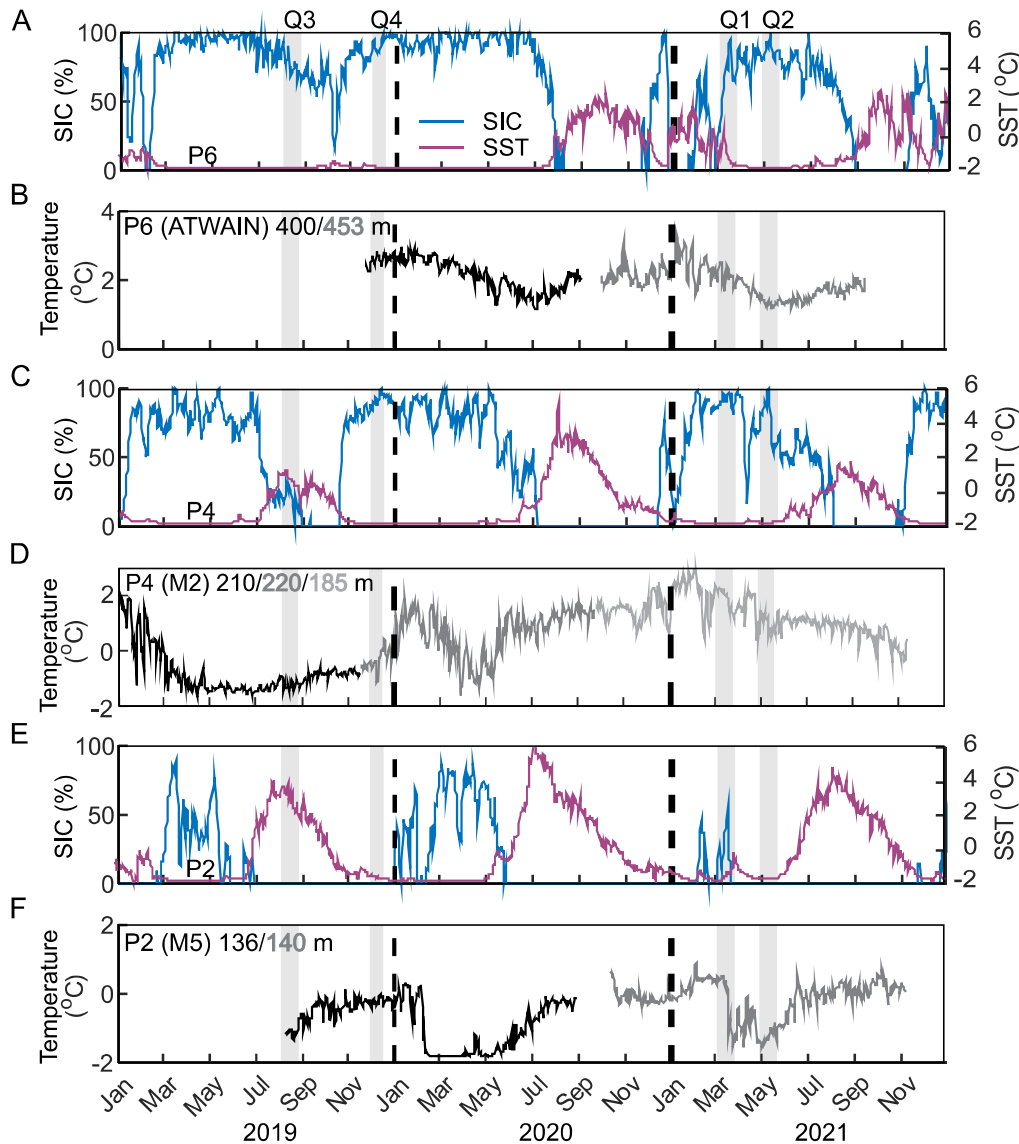


**Fig. 3.** Time series sea ice concentration (SIC), sea surface temperature (SST), and temperature at depth from three moorings that were deployed close to the present section on the continental slope (P6; A and B), in a trough (P4; C and D), and on a bank (P2; E and F). The vertical grey bands indicate the timing of the seasonal surveys.

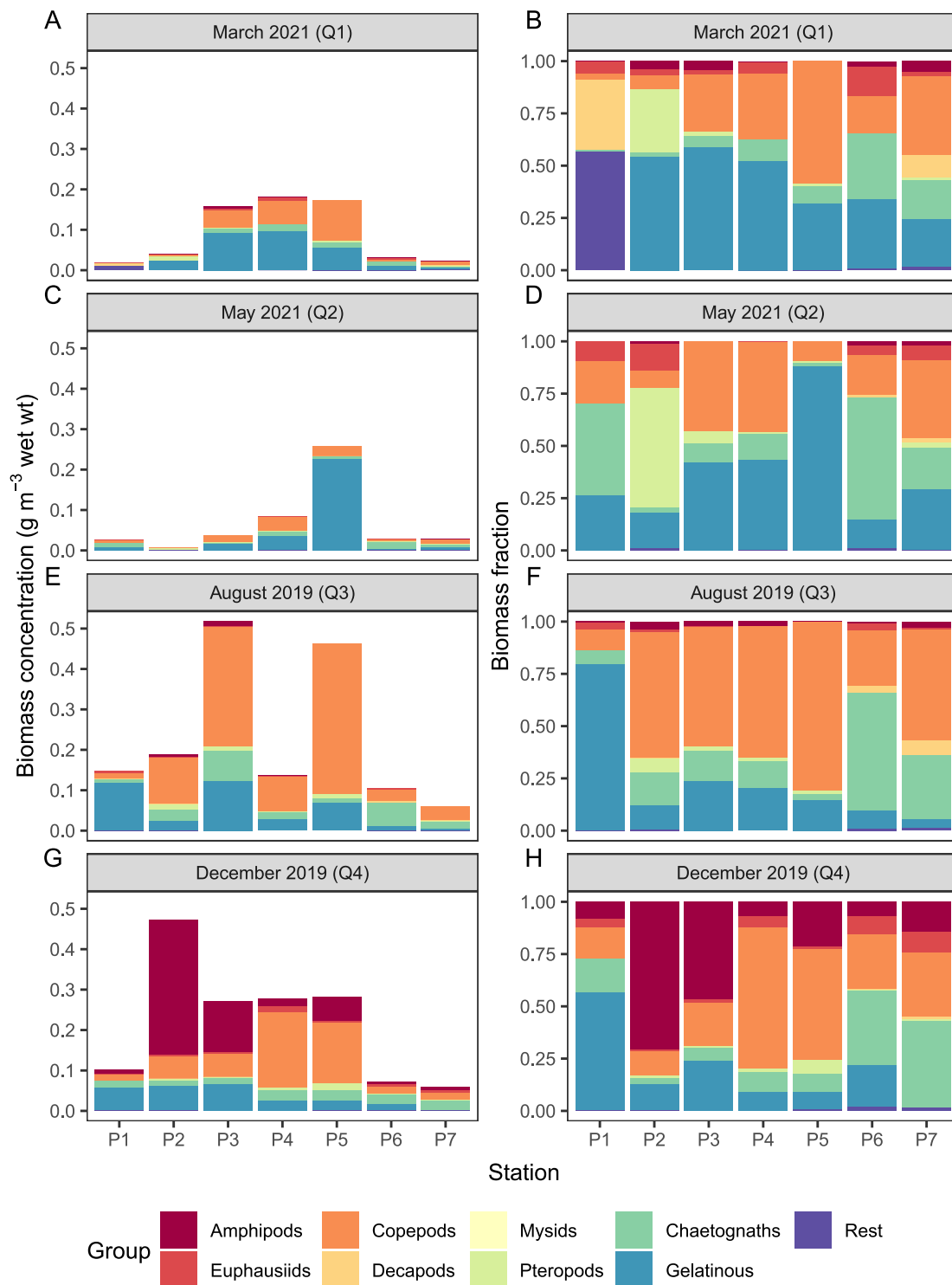


**Fig. 4.** Seasonality in biomass concentration (A, C, E, G) and as fractions of the biomass concentration (B, D, F, H) for the major groups along the South-to-North (P1-P7) section. Chaetognaths and other gelatinous zooplankton are treated as separate groups in this study. A similar figure based on area-normalized biomasses (Fig. S2) is available in the Electronic Supplement. Note that data on gelatinous plankton for P7 in cruise Q4 is missing.

Q3 (summer) than in the other seasons (Fig. 2).

There was also substantial temporal variation in the deeper water column, in particular at stations P2-P4 (Fig. 2). As opposed to the surface layers, these three stations were warmer in Q1 (winter) and Q2 (spring) than in Q3 (summer) and Q4 (early winter) (Fig. 2A-D), due to a clear shift of water masses at depth (Fig. 2, E-F and G-H).

### 3.2. Seasonal and interannual variability in ice and temperature

The seasonal surveys were conducted in 2019 (2 surveys) and 2021 (2 surveys), with a gap in 2020. This sampling gap may obscure seasonal dynamics by introducing year-to-year variability. To assess the impact of these temporal aspects, we combined data from multi-decadal time series of SIC (Fig. S6) with data on SST, SIC, and water temperature at depth from three moorings that were deployed in the vicinity of stations P6, P4 and P2 during the years 2019, 2020, and 2021 (Fig. 1, Fig. 3).

At P6, only a modest decrease in sea ice concentration took place before the Q3 sampling (August; Fig. 3A). Sea ice was present at P6 throughout the entire year of 2019, with a minimum in October, between the Q3 and Q4 samplings. The seasonal development in 2020 and 2021 was different from 2019. The sea ice vanished completely in August, causing the sea surface temperatures to rise to about 2 °C, and allowing for more light penetration into the water column. Consequently, at P6 the spring and summer bloom conditions of 2019 (as observed during the Q3 sampling) likely differed from the bloom situation in 2020 and 2021 (as observed during the Q2 sampling). The seasonal temperature development at depth at P6 did not mirror the surface conditions. Maximum temperature occurred in winter and minimum in spring or early summer (Fig. 3B), consistent with earlier studies (Ivanov et al., 2009, Renner et al. 2018). In contrast to the shallower station P4 (M2), the year-to-year variability in the temperature at depth was much less, and a regular seasonal pattern dominated overall variability in this signal (Fig. 3). Therefore, the sampling gap in 2020 will probably not be important in terms of temperature conditions at depth, for instance for seasonality of deep-water species. However, interannual temperature variation could exert a strong influence on the community in the surface layer.

At P4, the seasonal development of SIC and SST through 2019 and 2021 were relatively similar (Fig. 3C). This location was mostly ice covered from November-December to July (with short exceptions). The SST reached a maximum in August-September likely causing fairly similar light conditions in 2019 and 2021. However, the ocean temperature at depth near P4 varied considerably over the period 2019–2020 (Fig. 3D). The aforementioned shift between cold (IW and BSCDW) and relatively warm (wPW) water masses during Q1-Q4 (Fig. 2E-H) is visible and reveals stronger interannual than seasonal variability at this location.

At P2, the seasonal variability of SST was consistent through the 2019–2021 period, despite less sea ice in 2021 than in the two former years (Fig. 3E). At depth, temperatures were highest in winter (January-February) and reached a minimum in late winter or early spring (Fig. 3F). All in all, the seasonal cycle at P2 was fairly consistent through 2019–2021. However, considering the generally low SIC values at this station, it is questionable whether sea ice posed a limiting factor in terms of light availability to initiate and/or sustain average seasonal phytoplankton blooms, particularly in 2021.

### 3.3. Community composition of the large zooplankton in space and time

The taxonomic composition of the samples varied considerably with latitude and among surveys (Fig. 4). Biomass was dominated by only a

few taxa, such as *Calanus glacialis*, *C. hyperboreus*, *Themisto libellula*, *Beroe* spp., *Mertensia* spp. (see Fig. S1 for images), and several species of chaetognaths (including *Pseudosagitta maxima*, *Parasagitta elegans*, and *Eukrohnia hamata*), which are considered common to the Barents Sea (Fig. 4; Fig. S2).

In the northern Barents Sea (P2-P5), copepods contributed substantially to the total biomass in all seasons (Fig. 4). The Arctic copepods *Calanus glacialis* and *C. hyperboreus* dominated the overall copepod biomass along the section, particularly at the P3-P5 stations (Fig. 5A). The copepod biomass concentration was generally low at stations P6 and P7. The spatial patterns for *C. finmarchicus* are less clear, most likely owing to an under-sampling by the MIK net, in addition to the uncertainty in morphological identifying characteristics of *C. finmarchicus* and *C. glacialis* (Choquet et al., 2018). In addition, typically cold water associated species such as the three species in the genus *Paraeuchaeta* (*P. glacialis*, *P. barbata*, and *P. norvegica*) were also present though in lower quantities compared to the *Calanus* species. Other smaller copepod species, such as two species in the genus *Gaetanus* (*G. brevispinus* and *G. tenuispinus*) and *Metridia longa* were also found in very low quantities but are likely underrepresented in our samples due to the MIK's mesh size.

Euphausiids generally represented a minor portion of the total biomass for large zooplankton ( $0.003 \pm 0.003 \text{ g m}^{-3}$ ) in the Arctic waters of the Barents Sea (Fig. 4). The dominant euphausiid species were *Thysanoessa inermis* followed by *T. longicaudata* and *Meganycitiphanes norvegica* (Fig. 5B). The largest of the species, *M. norvegica* which is a typical Atlantic species, was present at most stations including the northernmost stations P6 and P7. The highest biomass concentrations of euphausiids were found in December 2019 and March 2021 (Q4 and Q1), while this group was almost absent in May 2021 (Q2). The subtropical and Atlantic/boreal euphausiid *Nematoscelis megalops* was observed occasionally in the region (Fig. 5B).

Amphipods were most dominant in terms of biomass ( $0.022 \pm 0.066 \text{ g m}^{-3}$ ) during early winter (Q4; Fig. 4). The Arctic pelagic amphipod *Themisto libellula* was by far the most abundant amphipod in the northern Barents Sea (Fig. 5C). Their biomass peaked sharply in early winter, and declined towards the end of winter, to very low biomass concentrations in spring. The more sub-Arctic species *T. abyssorum* (Kraft et al., 2013) was also present but in much lower concentrations. Higher biomasses for this species were associated with stations under Atlantic influence (P1, P6 and P7; Fig. 5C). Other amphipods such as *Apherusa glacialis* and *Eusirus holmii* (ice-associated) were encountered, but in comparatively lower concentrations.

Chaetognaths were present at all stations in all seasons. The highest biomass of chaetognaths was recorded in summer (Q3;  $0.032 \pm 0.025 \text{ g m}^{-3}$ ) and early winter (Q4;  $0.021 \pm 0.006 \text{ g m}^{-3}$ ) compared to winter (Q1;  $0.008 \pm 0.007 \text{ g m}^{-3}$ ) and spring (Q2;  $0.007 \pm 0.005 \text{ g m}^{-3}$ ; Fig. 4; Fig. 5D).

Gelatinous zooplankton generally contributed most to the biomass during late winter and spring (Fig. 4 and S2). Nevertheless, the highest average biomass concentrations were recorded in August ( $0.053 \pm 0.050 \text{ g m}^{-3}$ ). In December, the biomass varied between  $0.014 \text{ g m}^{-3}$  and  $0.065 \text{ g m}^{-3}$  at stations P1 to P6 (Fig. 5E). Individuals from the genera *Beroe* and *Mertensia* (both ctenophores) were the main contributors to the gelatinous plankton biomass at most stations and during all seasons. Other gelatinous zooplankton, *Aglantha digitale* and *Sarsia* spp. (both hydrozoans), also represented a considerable part of the biomass at some stations (Fig. 5E).

Larval fish were caught occasionally (Fig. S1). These were pooled into the “rest group” in Fig. 4. Note that larval fish are likely not representatively caught by vertical MIK net deployments.

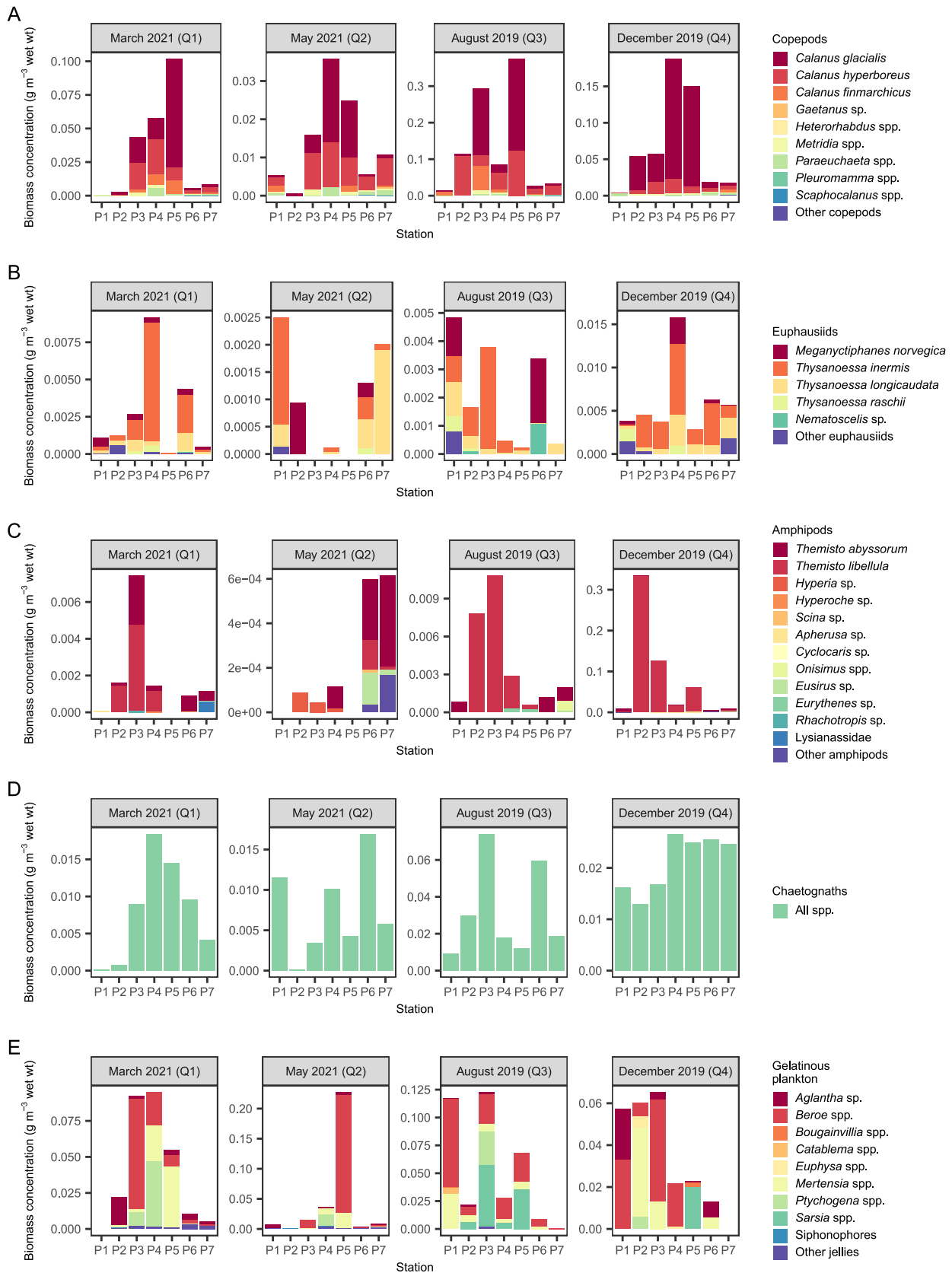


**Fig. 5.** Biomass concentrations ( $\text{g m}^{-3}$  wet wt.) of individual species/genera (A-E) per station (P1-P7) for the different seasons (left to right). Note that the y-axes have different scales. Chaetognaths (D) constituted by among others *Eukrohnia hamata*, *Parasagitta elegans*, and *Pseudosagitta maxima* were not quantified at the species level in our study. A similar figure based on area-normalized biomass is available in the Electronic Supplement (Fig. S3). Note that data on gelatinous plankton for P7 in cruise Q4 is missing.

### 3.4. Temporal variability in length distribution for selected species

The largest individuals of the dominant *T. inermis* were found in August (Q3, mean TL = 18.4 mm) followed by December (Q4, mean TL = 17.2 mm). The smallest size classes were recorded in March (Q1) and May (Q2), respectively 16.5 and 14.5 mm in the spring blooming period (Q2; Fig. 6A). The length distributions of the largest euphausiid *Meganycitiphanes norvegica*, spanned from 15 to 41 mm (N = 33, mean TL = 25.8 mm, std = 6.6) for all seasons combined. The smallest size classes were dominant in Q1 and Q2 seasons, with the largest ones in Q3 (Fig. 6D). The length-span of the more neritic species, *T. raschii*, ranged from 8 to 23 mm (N = 76, mean TL = 15.9, std = 3.3) and displayed no clear seasonal patterns (Fig. 6C). The smallest of the euphausiid species, *T. longicaudata* showed a similar length distribution (N = 379, mean TL = 11.85 mm, std = 1.3) for all four seasons (Fig. 6B).

In general, the amphipods showed several cohorts throughout the year, particularly *Themisto abyssorum* (N = 279, mean TL = 9.4, std = 2.9). The seasonal distribution in the length of *T. abyssorum* showed a similar pattern for Q1 and Q2 with somewhat larger individuals (ca. 10 mm) while Q3 and Q4 were skewed towards smaller sizes (mean TL ca. 8.8 mm; Fig. 6E). The number of *T. libellula* lengths measured was rather low in Q1 and Q2 (reflecting their abundances; Fig. 5C), hence, we only compared results between the Q3 and Q4 seasons (Fig. 6F). The length distributions in Q3 were skewed towards smaller values (mean TL 12.8 mm), and Q4 towards larger individuals (mean TL of 20.5 mm). In contrast to krill, the smaller individuals of *T. libellula* (3–6 mm) and adults with “marsupium” most likely indicate that spawning occurs in

this region. Note that both the smallest and largest individuals of euphausiids and amphipods are underrepresented in MIK catches.

### 3.5. Taxonomic and functional diversity

The Shannon-Weaver diversity index, which takes into account the taxon richness as well as their relative abundance, increased significantly with latitude (Linear regression model,  $t_{26} = 3.4$ ,  $p < 0.01$ ; Fig. 7A), and this effect did not vary significantly with season (ANCOVA:  $F_{3,20} = 1.4$ ,  $p > 0.05$ ). The number of water masses at each sample station had a significant positive effect on the Shannon-Weaver diversity (ANOVA,  $F_{2,25} = 8.9$ ,  $p < 0.01$ ). Pielou's evenness index did not vary significantly with latitude or season (ANCOVA:  $p > 0.05$  for all effects), nor with the number of water masses present at the station during sampling (ANOVA,  $F_{2,25} = 1.0$ ,  $p > 0.05$ ). Taxon richness exhibited a significant relationship with latitude (ANCOVA: covariate effect,  $F_{1,20} = 10.2$ ,  $p < 0.01$ ), but its sign differed per season (ANCOVA: interaction effect,  $F_{3,20} = 3.8$ ,  $p < 0.05$ ; Fig. 7B). The number of water masses from which the samples were taken had a significant effect on their taxon richness (ANOVA,  $F_{2,25} = 16.3$ ,  $p < 0.001$ ).

Diversity related variables were difficult to relate to other environmental variables. A positive relationship between the Shannon-Weaver diversity and bottom depth was only significant at the slope stations (P6 and P7; data not shown). Similar regression results were found for the taxon richness (data not shown). No relationship existed between Pielou's evenness and bottom depth (data not shown). In addition, only a very weak negative relationship existed between the Shannon-Weaver

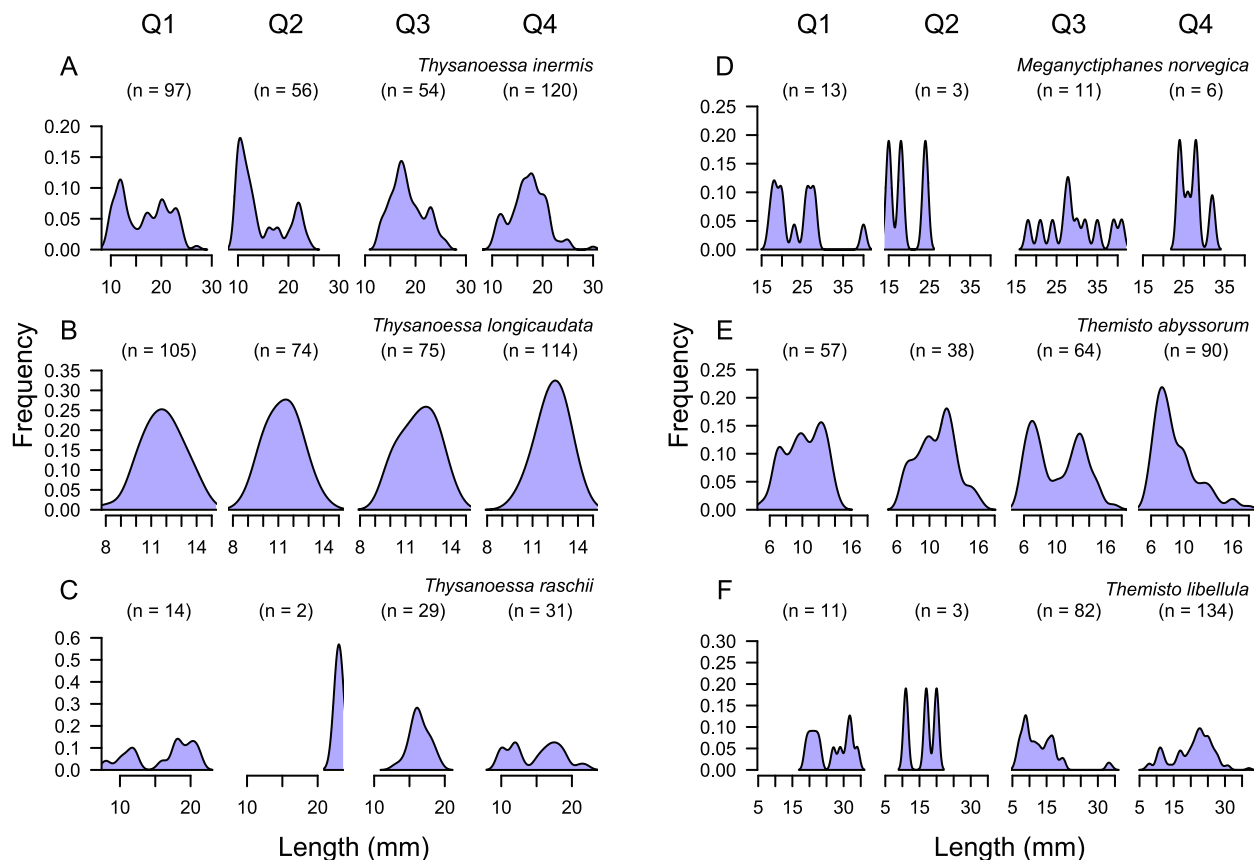


**Fig. 6.** Length (=total length, TL) distributions for the most abundant euphausiid (A-D) and amphipod species (E-F) per season (Q1-Q4). The blue areas are density estimates obtained using kernel smoothing (fixed bandwidth of 0.7 mm) of length counts from a randomized subsample of the MIK samples. The number of observations (n) are indicated above each graph.

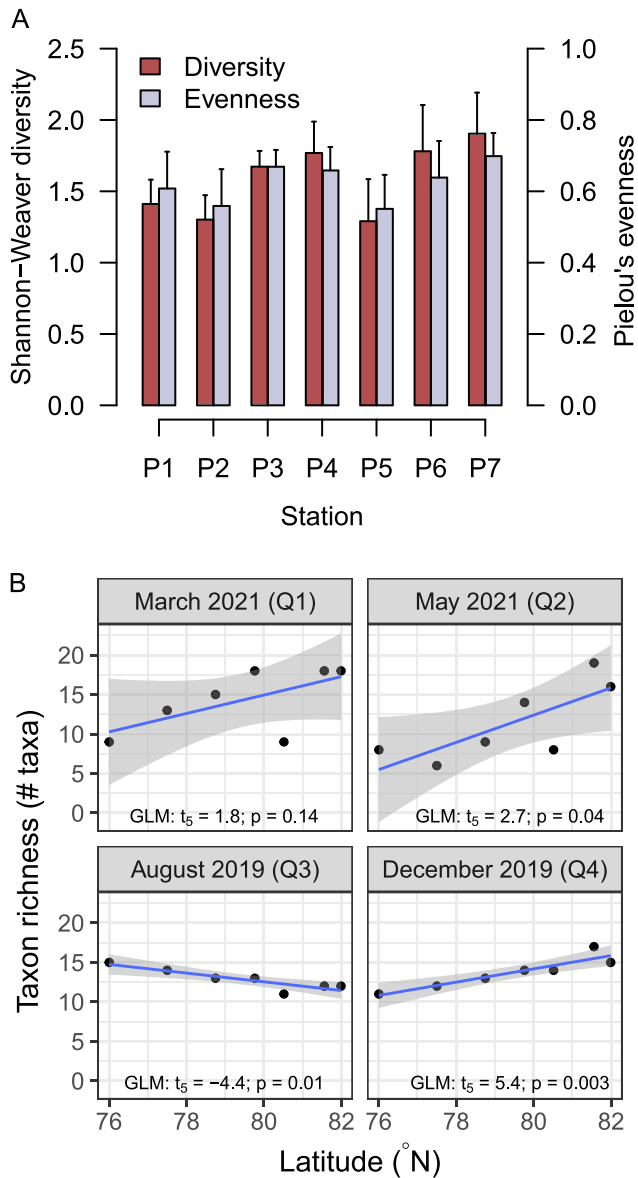


**Fig. 7.** Shannon-Weaver diversity index (red bars) and Pielou's Evenness (blue bars) along the sampling section (A), and taxon richness as a function of latitude (B) with an indication of the simple regression results. Taxa were included at the highest possible level.

diversity and the percentage of open water, independent of the season (Linear regression model,  $t_{26} = -2.1$ ,  $p < 0.05$ ; data not shown). No significant relationships existed between Pielou's evenness or the taxon richness and the percentage of open water (data not shown).

When the large zooplankton taxa were grouped according to their feeding guild, herbivores were dominant over most of the section in summer (Q3; Fig. 8). This group also includes detritivores because many species change their preference during certain parts of the seasonal cycle. Carnivorous zooplankton biomass (e.g. *Themisto libellula* and gelatinous plankton) was dominant in winter and spring in the southern part of the section (P2-P4 in Q1, P2-P5 in Q2, and P1-P3 in Q4). On the continental shelf (P1-P5) omnivorous zooplankton (e.g. *Meganyctiphanes norvegica*) contributions to the overall biomass were typically lower in most seasons. On the continental slope (P6 and P7), the proportion of omnivores seemed to be higher than on the shelf (Fig. 8). Also south of the Polar Front, omnivore biomass fractions tended to be slightly higher than in the northern Barents Sea, except in Q3 (Fig. 8). However, these

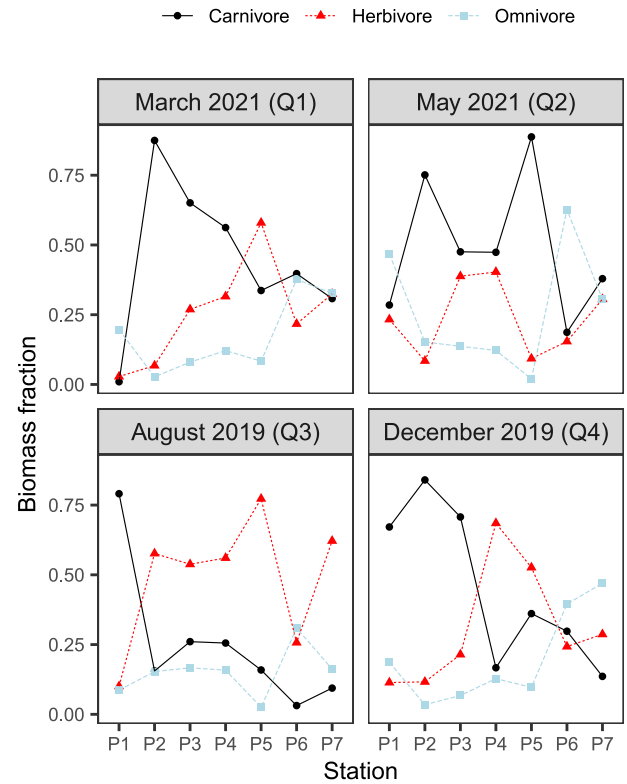


**Fig. 8.** Fractions of different feeding guilds in the total biomass per station and season. Note that the carnivores are underestimated at P7 in Q4 due to lacking gelatinous zooplankton data. See Table S1 for more details on the classification.

patterns are weak, most likely owing to the low sample sizes and sampling frequency.

### 3.6. Community structuring by environmental variables

Canonical Correspondence Analysis (CCA) of biomass concentrations for large zooplankton was performed using a forward selection procedure with different sets of environmental variables (Table S2), adding one environmental variable at a time, based on their explanatory power (Table 2), and low correlation to other included variables (Fig. S4). The final CCA model, representing 30% of the total inertia by its first three axes, included three significant environmental variables (shown as vectors in Fig. 9). As indicated by the angles between the environmental

**Table 2**

Results of the Canonical Correspondence Analysis (CCA) with one environmental variable at the time (Depth: bottom depth in m;  $T_{20m}$  and  $T_{150m}$ : depth-averaged temperature at 20 and 150 m depth [°C],  $S_{20m}$  and  $S_{150m}$ : depth-averaged salinity at 20 and 150 m depth [‰],  $\sigma_{0,20m}$  and  $\sigma_{0,150m}$ : depth-averaged potential density at 20 and 150 m depth [ $kg\ m^{-3}$ ]; %OW: percentage of open water area [%]; Chla: chlorophyll a concentration in the upper 50 m [ $\mu g\ l^{-1}$ ]; Latitude in °N). The p-values are based on 20,000 permutations.

Model	p	Explained variation (%)
Species ~ log(Depth)	< 0.001	13.5
Species ~ log( $T_{150m}$ )	< 0.001	13.8
Species ~ $S_{150m}$	< 0.001	10.8
Species ~ $\sigma_{0,20m}$	< 0.001	9.3
Species ~ $S_{20m}$	< 0.01	9.2
Species ~ log(Chla)	< 0.01	7.9
Species ~ Latitude	0.11	5.4
Species ~ log( $T_{20m}$ )	0.28	4.4
Species ~ $\sigma_{0,150m}$	0.62	3.3
Species ~ log(%OW)	0.97	1.9

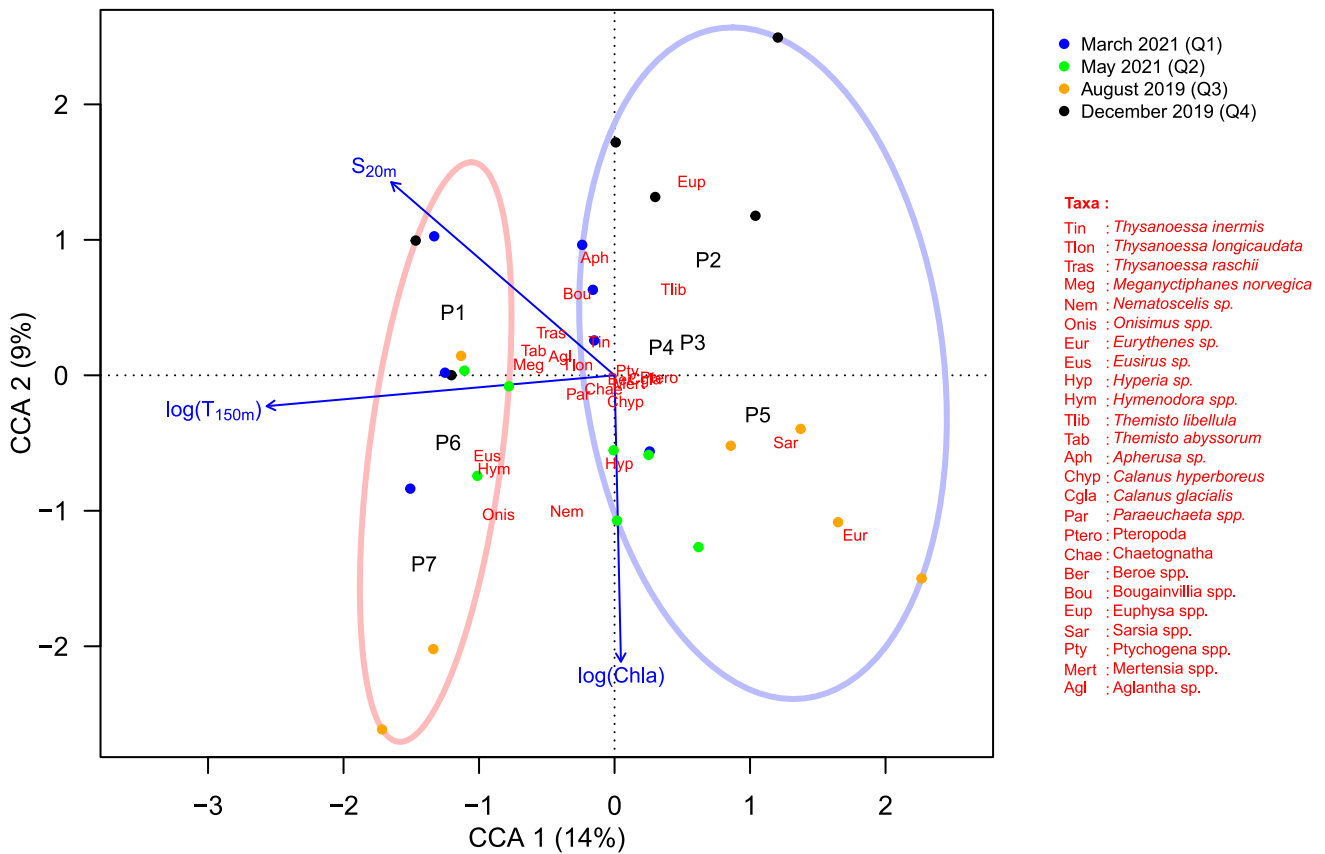


**Fig. 9.** Canonical Correspondence Analysis (CCA) using species or genera for most zooplankton. Included environmental variables are the temperature at 150 m depth (log-transformed; average temperature over the depth range of 145 to 155 m), Chl *a* (log-transformed) and salinity in the upper layer (average over a depth range from 15 to 25 m). Observations are presented as colored dots where the color indicates the season (cf. legend). Ellipses indicate a separation between stations/observations with Atlantic Water (red) and the true northern Barents Sea stations (blue). The first three axes were significant. The first two axes represented 23% of the variability in the data set. Results of a similar analysis with bottom depth instead of  $T_{150m}$  are available in the Electronic Supplement (Fig. S5). Note that station P7 for cruise Q4 was excluded from the CCA analysis due to missing data on gelatinous plankton.

vectors and the CCA-axes, the temperature of the water column interior ( $T_{150m}$ ) was strongly associated with the primary axis (CCA1). This variable could be replaced by bottom depth in the analysis, with virtually the same resulting structure (Fig. S5). Salinity in the surface layer ( $S_{20m}$ ) exhibited an association with CCA1, CCA2, as well as CCA3 (data not shown for CCA3). The chlorophyll *a* concentration (Chl *a*) was mainly associated with CCA2. Despite the significance of Chl *a* in this analysis, no clear relationships with biomass concentrations of any individual species were found (data not shown).

The observations (dots in Fig. 9) fell into (1) a group with Atlantic influence (red ellipse), and (2) a northern Barents Sea group (blue ellipse). The Atlantic group contained observations from stations P1, P6, and P7. Station P1 is the only station in the section that resides south of the Polar Front in (modified) Atlantic Water (Fig. 1). The northernmost stations P6 and P7 are generally ice-covered (see Fig. 1B) but have Atlantic Water in deeper waters (below 100–200 m depth, Fig. 2). These stations contained, in addition to Atlantic taxa (*Meganctiphanes norvegica*, *Thysanoessa longicaudata*, and *Nematoscelis* spp.), the sub-Arctic amphipod, *Themisto abyssorum*, deep water taxa (*Hymenodora* spp.), and ice-associated taxa (*Onisimus* spp., *Eusirus* spp.). This Atlantic/deep-water/ice-associated group (hereafter referred to as Atlantic group) was associated with higher temperatures at 150 m depth (positive direction of the  $T_{150m}$  vector in Fig. 9).

The northern Barents Sea group (stations P2-P5; blue ellipse) was associated with colder water at depth (negative direction of the  $T_{150m}$  vector in Fig. 9), typical cold-water taxa such as *Themisto libellula*, *Calanus hyperboreus*, and the deep-water species *Eurythenes* sp. Black and blue dots (Q4 and Q1) tended to be located towards higher surface

salinities and lower Chl *a* values, whereas green and orange dots (Q2 and Q3) grouped at higher Chl *a* values and lower surface salinity. This may be largely a seasonal factor considering the seasonality in these two variables. It suggests that seasonality plays an important - though secondary-role (Fig. 9). Note, however, that we cannot fully distinguish seasonality from year-to-year variation with our sampling scheme.

Repeating the CCA with all stations on all surveys, while excluding all gelatinous taxa, provided the same overall results (data not shown). Generally, a much higher sample size would be needed for robust statistical analyses of the community of large zooplankton than we applied in this study. Hence, these results should be interpreted carefully.

## 4. Discussion

### 4.1. Spatio-temporal patterns and the role of key species

Two copepod species, *Calanus glacialis* and *Calanus hyperboreus*, were major components of the large zooplankton community in the central part of the transect. Both species occurred along the larger part of the transect. A tendency seemed to exist toward the dominance of *C. glacialis* at the shelf stations in the northern Barents Sea and *C. hyperboreus* on the continental slope and in the Arctic Ocean (see Fig. 5 and S3 in the Electronic Supplement). However, because of the small size of *C. glacialis* relative to the mesh size of the MIK net, caution is needed in quantitatively interpreting our biomass values for this species. This contrast between shelf and slope in our zooplankton samples was confirmed by data from Multinet samples (0.25 m<sup>2</sup> opening, 180  $\mu$ m) taken during the same cruises (presented in Wold et al., 2023), and agrees with the

common perception of *C. hyperboreus* and *C. glacialis* as deep-water and shelf-associated species, respectively. However, this contrast may be more related to prevailing sea ice parameters than to bathymetric factors (Ershova et al., 2021). The same reservation about size selectivity of the MIK with regard to copepods applies to the even smaller *C. finmarchicus*, for which no clear spatial pattern was observable in our samples. However, from the aforementioned Multinet samples, we know that the Atlantic *C. finmarchicus* was most abundant at P1, P6 and P7, with Atlantic influence, whereas the Arctic *C. glacialis* generally dominated at stations with polar influence, P2-P5 (data not shown). Assuming a water content of 74% (Ikeda and Skjoldal, 1989), the area-normalized biomass of the copepods in our samples was in spring (Q2) and summer (Q3) of the same order of magnitude as those reported by Mumm et al. (1998; reported as dry mass) for the Barents Sea in summer. Dalpadado et al. (2014) reported mesozooplankton biomasses (dry mass) for the northern Barents Sea based on several years of data that were similar to ours, assuming the same value of 74% for water content. Our copepod biomasses from the shelf break (P6, P7) in summer (Q3) also fell within the range reported by Kosobokova and Hirche (2009) for the same region.

Comparison of our MIK samples with euphausiid and amphipod catches from a macroplankton trawl in waters around Svalbard (Knutsen et al., 2017) showed that the catch biomass proportions of euphausiids (60% *Thysanoessa inermis* vs. 40% *Meganctiphanes norvegica*) and amphipods (88% *Themisto libellula* vs. 12% *T. abyssorum*) were strikingly similar. As expected, our study extending into high Arctic waters contained higher concentrations of cold-water amphipod species *T. libellula* and lower euphausiid concentrations than reported by Knutsen et al. (2017). Euphausiids represented a minor portion of the biomass in the Arctic waters of the Barents Sea.

A recent study conducted very close to the stations reported in our study (P5, P6, and P7) found low euphausiid and larval fish abundances in the high Arctic waters, even when using a larger modified (to be used in ice covered waters) pelagic and specially designed macroplankton trawls (Ingvaldsen et al., 2023). Previous studies in the Barents Sea have also confirmed that, unlike the large pelagic amphipods, the Atlantic/boreal euphausiids do not penetrate the Arctic waters and are rarely found north of the Polar Front (Dalpadado and Skjoldal, 1996). Furthermore, the distribution of Atlantic/boreal euphausiid species in the Arctic waters seems to be mainly restricted to the deeper (>200 m) Atlantic waters (Dalpadado et al., 2008a). Even with the ongoing “borealization” of the Barents Sea and euphausiids expanding their distribution further north (see also below), results so far seem to indicate that they do not enter much into the colder waters in the north (ICES, 2021). The above studies seem to corroborate our findings, that there are fewer euphausiids and larval fish in the region compared to jellyfish, chaetognaths, and Arctic amphipods.

The hyperiid amphipod *Themisto libellula* is an important component of Arctic pelagic ecosystems (Auel et al., 2002), and a key prey of polar cod *Boreogadus saida* (Dolgov et al., 2011; Dalpadado et al., 2016; Kohlbach et al., 2017; ICES, 2021). In our study, *T. libellula* dominated the amphipod catches in the northern Barents Sea, with a peak in early winter (Q4). However, at the end of winter (Q1), their biomass was very low, which was surprising considering their 2- to 3-year life expectancy (Koszteyn et al., 1995; Dale et al., 2006). It is possible that this species was under-sampled at certain stations or seasons due to their swarming behavior near the bottom (Vinogradov, 1999). A more plausible explanation may be found in the difference in ice conditions between 2019 and 2021. *T. libellula* is a true cold-water species, and a positive relationship between multi-year fluctuations in ice cover and *T. libellula* abundance exists (Dalpadado, 2002; Stige et al., 2019a). The low ice concentration in 2021 relative to 2019 may provide at least in part an explanation for the sharp decrease from Q4 to Q1. Therefore, the strong difference in *T. libellula* biomass between Q4 and Q1 may to a large extent be a year-effect, rather than seasonal dynamics. *T. libellula* is predominantly carnivorous, preying mostly on mesozooplankton including copepods (Auel et al., 2002; Dalpadado et al., 2008b). The

presence of adults with marsupium and young individuals (ca. 4–6 mm – see Fig. 6 and Fig. S1 in the Electronic Supplement) in our study suggests reproduction in this region. The abundance of *T. libellula* in the northern Barents Sea has decreased over the years, with the suggested explanation being a reduced coverage of Arctic water masses (Stige et al., 2019a).

The ongoing “borealization” of the Barents Sea has large implications for the key zooplankton species and their predators in the region. As a result of warming, Atlantic/boreal zooplankton species have expanded their distribution further north, which would benefit major planktivorous fish species, such as capelin, in the Barents Sea. Many recent studies have shown that euphausiids in the Barents Sea have extended their distribution further north (ICES, 2021 and references therein) compared to earlier periods (Dalpadado and Skjoldal, 1996; Zhukova et al., 2009; Orlova et al., 2015). Two specimens of *Nematoscelis megalops* were observed in station P6 in winter 2021 (81°N), which until recently has been almost absent in the Barents Sea (Zhukova et al., 2009). However, the low abundance of euphausiids in our study indicates that they are not yet established in the Arctic. At the same time, Arctic and sympagic fauna are experiencing decreasing sea ice and a diminishing area of Arctic waters (Dalpadado et al., 2020; Ingvaldsen et al., 2021). The retreat of sea ice will have a negative impact on associated fauna due to the loss of habitat and ice algae as food source. We consider it likely that these conditions are reflected by the generally few ice-associated amphipods (sympagic and Arctic) observed in our study - except for the winter survey in 2021.

Gelatinous zooplankton taxa were present at all stations and all seasons. *Beroe* spp., *Mertensia* spp., and *Sarsia* spp. made up the bulk of the gelatinous plankton biomass in our northern Barents Sea samples. For many gelatinous zooplankton species in the area, the distribution ranges are unknown due to a lack of studies. Some species showed clear Arctic/Atlantic preference, however. For instance, *Aglantha digitale* and *Bougainvillia* spp. were mainly found at stations with some Atlantic influence. This agrees with the findings from Maňko et al. (2020), who focused on the Fram Strait, and confirms the importance of water mass characteristics in structuring this zooplankton community.

Chaetognaths also contributed notably to the biomass in the study region and were present at most stations. We observed the highest biomasses in summer and early winter. Hop et al. (2021) also reported high contributions of chaetognaths and ctenophores to the zooplankton community north of Svalbard. The species *Eukrohnia hamata*, *Parasagitta elegans*, and *Pseudosagitta maxima*, were identified in our samples, but chaetognath identification to species level was not systematically done throughout the different surveys. Considering the differences in their life-history characteristics and feeding ecology, and the expected differences in sensitivity to a changing Arctic ecosystem (Grigor et al., 2014, 2017, 2020), future surveys would benefit from a more in-depth treatment of this group.

#### 4.2. Drivers of large zooplankton community composition

The Arctic ecosystem is generally perceived as having relatively low diversity, compared to other marine ecosystems (Gradinger et al., 2010). In our study taxonomic diversity varied only weakly with latitude along the studied section. However, a strong effect existed from the number of water masses present during sampling on the observed diversity and taxon richness. This can be understood as an effect of habitat heterogeneity and/or as a direct transport effect, considering the different origins of these water masses (Atlantic vs. Arctic). The weakness of the observed latitudinal diversity gradient might be explained by the relatively short latitudinal range of the sampled transect, and the presence of Atlantic water at the southernmost station (P1), at the intermediate station P4 (in Q2), and on the two northernmost stations (P6 and P7). Atlantic species were present in the south and in the north, while the community composition at the shelf stations in the middle of the transect (P2-P5) had a stronger Arctic component.

On the continental slope diversity was associated with bottom depth, most likely owing to the inclusion of deep-water and ice-associated species at these stations (see also below). Depth-dependence of diversity indices was also demonstrated for the deep Arctic Ocean by Kosobokova et al. (2011). Their depth-resolved Multinet data showed the highest diversity in layers with Atlantic Water. Although our data are not vertically stratified, the observed weak and positive relationship between diversity and bottom depth might reflect increased diversity in Atlantic Water, which is transported eastward at intermediate depth along the continental slope (i.e. at P6 and P7).

The biomass of the large zooplankton in the northern Barents Sea was dominated by only a few species that establish food web links, transferring energy from primary production to higher trophic levels, such as capelin, cod, polar cod, whales, and seabirds (Orlova et al., 2013; Michalsen et al., 2013; Ressler et al., 2015). In line with the water mass effects on taxon diversity and richness, our Canonical Correspondence Analysis also identified the water mass distribution as one of the most important structuring factors of the sampled zooplankton community. This confirms our hypothesis and agrees with the findings of Hop et al. (2021), who also reported a dominant influence of water mass characteristics and water depth in structuring the zooplankton community over the Yermak Plateau, north of Svalbard. Flores et al. (2019) also reported an important role of water mass in structuring the under-ice fauna at the larger scale of the Eurasian Basin. In our study, Atlantic, deep-water, and ice-associated zooplankton taxa grouped together, and fell into the group of stations that consisted of the most southern station (P1) and the two most northern stations over the continental slope and Arctic Ocean (P6 and P7). These stations were hydrographically characterized by a contribution of warm Polar Water (wPW), and (modified) Atlantic Water (AW/MAW). However, the slope stations, P6 and P7, were also characterized by deep water, which explains the similarity between our ordinations based on water mass characteristics and bottom depth.

The northern Barents Sea stations (P2-P5) were associated with a colder water column and typical Arctic taxa. Of these northern Barents Sea stations, P4 somewhat stood out by exhibiting (weak) Atlantic signals, both in hydrography (wPW) and the presence of Atlantic species, such as *Aglantha digitale* and the sub-Arctic species *T. abyssorum*. This is likely due to Atlantic water that is transported southward along the channel west of Franz Josef Land (Lind and Ingvaldsen, 2012). Despite the large overlap in geographic distribution between *T. abyssorum* and *T. libellula*, *T. libellula* is largely confined to cold water masses (although adaptation of local populations has been observed), whereas *T. abyssorum* displays a wider temperature tolerance (Percy, 1993; Havermans et al., 2019). A recent study by Kaiser et al. (2022), illustrated a stronger response in activity of *T. abyssorum* to higher temperatures, as compared to *T. libellula*, which was by these authors interpreted as a potential competitive advantage of the former over the latter under a scenario of continued Arctic warming.

Our study also suggests that surface salinity and the Chl *a* concentration were significant structuring factors of the large zooplankton community. However, in this study these represent mainly a temporal component, consisting of a mixture of year-to-year and seasonal effects.

Sea ice is often implied as a structuring variable in Arctic faunal communities (e.g. David et al., 2015; Flores et al., 2019; Ehrlich et al., 2020). Though the sea ice concentration (SIC) or its complement, the percentage of open water (%OW), did not emerge as a strong structuring variable for the sampled zooplankton community in our study, these variables play an important role for sympagic organisms. At the level of individual species, sea ice (living habitat) can play an important role in their life-history. For example, *Eusirus holmii*, *Onisimus* spp. and *Apherusa glacialis* are associated with sea ice for at least part of their life cycle (Macnaughton et al., 2007). In our CCA, *Eusirus* spp. and *Onisimus* spp. grouped together with the Atlantic and deep-water species. These truly

sympagic species were only found on the two most northern stations, whereas *A. glacialis*, which is less associated with sea ice (Arndt et al., 2005; Kunisch et al., 2020), was also found on the continental shelf of the northern Barents Sea. It is possible that it is the dominance of seasonal ice along the sampled transect and the proximity of perennial ice north of the continental slope that largely restricts the distribution of these truly sympagic species to P6 and P7, whereas *A. glacialis* may occur more easily in seasonal ice further south along the transect. Note that sympagic organisms are under-represented in our samples due to the vertical deployment of our ring net, which is not adapted to sample close to the ice-water interface. This likely caused an under-sampling of the sympagic fauna.

#### 4.3. Seasonal or interannual variability?

Sampling a full seasonal cycle within a period of one year was not possible due to the COVID situation. Hence, it was necessary to assess the potential impacts of year-to-year variability on our seasonal analysis. We have attempted to assess this impact by investigating water column temperature (at the surface and in the interior water column) and sea ice conditions based on mooring time series and satellite-derived data. Considering the documented long-term trends in these variables and their impact on ecosystem functioning (e.g. Carmack and McLaughlin, 2011; Barber et al., 2015), they at least enable us to assess the similarity of the years 2019 and 2021, and how typical these years are compared to long-term trends (Fig. S6).

Substantial ice loss has occurred in the Barents Sea since the late 1970s (Onarheim et al., 2018), but a moderate recovery has been observed since the warming peaked in 2016 (Ingvaldsen et al., 2021). Consequently, the northwestern Barents Sea experienced a rather extensive sea ice cover in 2019 (Fig. S6), particularly in late summer, which even had substantially more ice than the 1979–2021 average. Also, 2020 had extensive sea ice cover, mostly in winter. In 2021, the sea ice area decreased to below the long-term average, although still higher than most of the years during the 2012–2016 period (Fig. S6). Thus, our surveys were conducted in relatively rich sea ice years, in a long-term perspective.

The northern Barents Sea, as well as other regions at high latitudes, has a highly seasonal primary production regime and organisms have evolved in response to the short and intensive productive season and low food supply the rest of the year (e.g. Falk-Petersen et al., 2009; Wassmann et al., 2011). In addition, there is strong interannual variability in the timing and strength of the seasonal cycle (Dalpadado et al., 2014; Stige et al., 2019b), reflecting that the northern Barents Sea is an outer marginal ice zone already strongly influenced by warming and sea ice loss (e.g. Wassmann et al., 2011). The pronounced interannual differences in water column temperature during 2019–2021 revealed that it is not feasible to combine the four seasonal surveys Q1-Q4 into a full annual cycle for the entire studied section (Fig. 3). Therefore, our sampling does not permit us to distinguish seasonality from year-to-year variability in organisms that are at the limits of their temperature tolerance or substantially affected by temperature in their growth. The presence of a year-effect in our data is also supported by the resemblance between Q1 and Q2, and between Q3 and Q4 in terms of overall biomass concentrations and length distributions of key species, which suggest at least to some extent a year effect rather than a seasonal effect. The data are well suited for assessing seasonal development from late summer (Q3) to early winter (Q4), and from late winter (Q1) to spring (Q2). However, the transition/difference from early winter (Q4) to winter (Q1) and from spring (Q2) to summer (Q3) cannot be considered seasonal progression. Nevertheless, our dataset presents a winter situation (Q4) with zooplankton biomass concentrations comparable to the summer situation (Q3). Studies from the Atlantic Arctic inflow have

revealed that the levels and biological interactions across most trophic levels are higher in winter than previously known (Berge et al., 2015; Hobbs et al., 2020), but data from the winter situation are rare.

#### 4.4. Trophic relationships in the zooplankton community

Our study found seasonally varying contributions of different feeding guilds in the biomass of the large zooplankton in the northern Barents Sea. The contribution of herbivores to the zooplankton biomass in the northern Barents Sea stations (P2-P5) during summer (Q3) was higher than that of carnivores or omnivores. Note that this evaluation was based on the biomass composition of the large zooplankton, combined with an assignment to feeding guild based on literature. It was not based on analyses of gut contents. Hence whether the species that we consider as omnivores in reality performed omnivorous, carnivorous, or herbivorous feeding activity at the moment of sampling remains unresolved. Outside the productive season carnivores dominated the sampled zooplankton biomass on the continental shelf of the northern Barents Sea. Kohlbach et al. (2021) observed an increase in carnivory fatty-acid markers from summer (Q3) to winter (Q4) in *T. abyssorum*, *T. libellula*, and even in *C. finmarchicus*. For the latter, they interpreted this as a sign of continued feeding in winter. Also relevant in the food-web context, Geoffroy et al. (2019) studied seasonal macroplankton/fish composition and their trophic links north of Svalbard, and suggested a *Calanus*-based food-web in summer and a krill-based food-web in winter. The seasonal alteration between carnivores and herbivores, and between top-down and bottom-up control is a common property of the Arctic and Antarctic ecosystems (Hunt et al., 2011).

The Arctic food web exhibits weak trophic connectivity (de Santana et al., 2013; Kortsch et al., 2019; Sivel et al., 2021; Wassmann et al., 2020; Kortsch et al., 2015; Planque et al., 2014). Our study found some indications for positive or negative correlations between biomass concentrations of some predator and prey species, but always with large uncertainty. Such correlations are sometimes interpreted as indications of top-down (negative correlations) or bottom-up (positive correlations) control (e.g. Dalpadado et al., 2020). Ideally, this type of analysis is based on long-term variation recorded in time series (e.g. Stige et al., 2019a), but a spatial dimension has also been used (e.g. Kortsch et al., 2019). During early winter the latitudinal distributions of *Themisto libellula* and *Calanus hyperboreus*, seemed to suggest a spatial mismatch between a predator and its main prey, with a maximal *T. libellula* biomass concentration further south than the biomass concentration maximum of the copepods (data not shown). However, this could not be consolidated by statistical testing, most likely due to a combination of low observation numbers, size selectivity of the MIK net, and limited sampling volumes. A more in-depth study focusing on trophic interactions is required to arrive at solid conclusions.

Weak trophic connectivity may result from the strategy to build up energy reserves for bridging a food-deprivation period in winter. Herbivores such as *Calanus glacialis* and *Calanus hyperboreus*, and carnivores such as *T. libellula* and *Mertensia ovum* store varying amounts of lipids and wax-esters, enabling them to survive periods of food deprivation and to (partially) fuel reproduction in winter or early spring (Percy and Fife, 1981; Scott et al., 2000; Auel et al., 2003; Falk-Petersen et al., 2009; Noyon et al., 2011). In addition, weak trophic links may emerge from seasonal changes in diet. Our results seem to indicate that at some locations omnivorous species became more important in terms of biomass at the expense of carnivorous species in line with results from a study by Kortsch et al. (2019), which covered the entire Barents Sea. Omnivory under the form of seasonal switching between herbivory and carnivory, e.g. for euphausiids (Kaartvedt et al., 2002; Dalpadado et al., 2008b; Cabrol et al., 2019) and chaetognath species (Grigor et al., 2017, 2020), has been related to survival and/or reproductive success of these individual species under uncertain environmental conditions. *Meganycitophanes norvegica* may be more sensitive to bottom-up control due to copepod availability in winter than *Thysanoessa* spp., whereas the latter

makes more extensive use of lipid reserves to bridge this period of food deprivation (Cabrol et al., 2019). Grigor et al. (2017) suggested that the growth of the chaetognath, *Eukrohnia hamata*, might be enhanced under an extended bloom period relative to *Parasagitta elegans* due to its seasonal switch to phytoplankton and detritus. Such flexibility in trophic links and food demands may render the Barents Sea more resilient towards expected climate change (Renaud et al., 2018).

#### 4.5. Limitations of the study and future perspectives

This study of the community of large zooplankton was based on vertical hauls with a MIK net. This net does not quantitatively capture smaller species because of its mesh size, while large-bodied fast swimming taxa will have a higher possibility of escaping the net due to the relatively small mouth opening compared to that of a macroplankton trawl. However, as discussed, the reported patterns in our data agree well with previous studies, supporting the validity of our conclusions. The statistical power of our analyses is limited by the relatively few observations and might have been further restrained by the restricted filtration volumes from the vertical hauls of the ring net. In addition, ice-associated taxa may be under-represented in vertical hauls in open spots where the ice was removed by the ship. Another aspect is that larger sampling volumes obtained by larger trawls, i.e. greater sampling effort, will increase the likelihood of encountering individuals of “rare” taxa and taxa with patchy distributions. Future surveys should use dedicated macrozooplankton trawls in the ice if the survey platform permits. Analyses of echosounder and ADCP data could provide useful additional information on the zooplankton vertical distribution, relative abundance, and seasonality.

Our results showed an Atlantic character at the southern station, and a combination of Atlantic, Polar, deep-water, and sea ice-related characteristics at the northernmost stations. Deep-water species from the continental slope were caught together with the sympagic species and fauna of Atlantic origin. A northward extension of the transect into perennial ice, covering a larger part of the deep Polar Ocean, could provide the resolving power needed to identify individual effects of bottom depth, water mass, and seasonal vs. perennial ice. Such an extension would cut across the Eurasian Basin and therefore allow for the investigation of contrasts among several of the domains in the conceptual model of the contiguous domains, put forward by Wassmann et al. (2020). Linking survey design to such pan-arctic conceptual models may enable us to address knowledge gaps more efficiently. Water mass characteristics have been identified by several independent statistical studies as the primary shaping factor in the taxonomic structure of the zooplankton community (e.g. Flores et al. 2019; Hop et al. 2021; this study). Although largely descriptive in nature, such studies guide future research focus to illuminate the exact underlying mechanisms that produce the observed patterns. For example, the study by Kaiser et al. (2022) suggests that certain key zooplankton species in the Arctic are tolerant enough to cope with higher temperatures as expected under a continued borealization process but may not be competitive enough compared with their Atlantic congeners. The observed patterns in our studies may therefore partly be the result of competitive outcomes, rather than shifting environmental factors away from the tolerance windows of these species. Studies that focus on the underlying mechanisms may provide equations to test our pan-arctic conceptual model (Wassmann et al., 2020).

## 5. Conclusions

This study initiated by the Nansen Legacy Project, provides a snapshot of the community composition in the northern Barents Sea and neighboring continental slope for different seasons of 2019 and 2021. It adds to a growing body of ecological data that is required to deepen our understanding of this rapidly changing ecosystem.

We investigated the community structure of the larger zooplankton

in the northern Barents Sea in relation to environmental variables. Our data showed that the large zooplankton in the northern Barents Sea exhibits a marked spatial structure and consists of a relatively small number of typical cold-water species associated with Polar Water masses. Atlantic Water transport adds allochthonous species, mainly at the southern (Polar Front) and northern (continental slope) boundaries of the studied region. As such, Atlantic Water transport increases the overall diversity of this Arctic system. Considering the projected warming and Atlantification of the Barents Sea and the Arctic, one could hypothesize a shift from a dominance of cold-water species towards more warm water-associated southerly taxa over time.

Our results showed that temperature and bottom depth were the most important variables influencing community composition of the large zooplankton, followed by upper layer salinity and Chl *a*. Chl *a* is highly inversely correlated with nutrients in the Barents Sea (Dalpadado et al., 2020), which makes our study consistent with earlier investigations showing nutrients and sea-ice properties to be the main drivers of an Arctic epipelagic zooplankton community structure (Flores et al., 2019).

The biomass of the large zooplankton in the northern Barents Sea exhibits a seasonal cycle with strong relative contributions of typical carnivores in winter and more herbivores in summer, suggesting seasonally alternating top-down and bottom-up control. This agrees with results from earlier studies and is considered an ecosystem property that facilitates coping with the strong seasonality in primary production.

#### Declaration of Competing Interest

The authors declare that they have no known competing financial interests or personal relationships that could have appeared to influence the work reported in this paper.

#### Data availability

The zooplankton data is available with the following link: <https://doi.org/10.21335/NMDC-1549427017>

#### Acknowledgments

We gratefully acknowledge Øyvind Lundesgaard for providing mooring data. We thank the BESECO project for allowing us to use the functional trait database, and Angelo Ciambelli for helping with the identification of the gelatinous plankton species. Thor Klevjer is acknowledged for reading through an earlier version of the manuscript. We are grateful to the three anonymous reviewers for their valuable comments on the manuscript. This study made use of E.U. Copernicus Marine Service Information (<https://doi.org/10.48670/moi-00165>). The research was performed within the framework of the Nansen Legacy project (RCN-276730), funded by the Research Council of Norway.

#### Appendix A. Supplementary material

Supplementary data to this article can be found online at <https://doi.org/10.1016/j.pocean.2023.103065>.

#### References

- Arndt, C.E., Berge, J., Brandt, A., 2005. Mouthpart-atlas of Arctic sympagic amphipods - Trophic niche separation based on mouthpart morphology and feeding ecology. *J. Crustac. Biol.* 25, 401–412. <https://doi.org/10.1651/C-2544>.
- Arrigo, K.R., van Dijken, G.L., 2015. Continued increases in Arctic Ocean primary production. *Prog. Oceanogr.* 136, 60–70. <https://doi.org/10.1016/j.pocean.2015.05.002>.
- Auel, H., Harjes, M., da Rocha, R., Stübing, D., Hagen, W., 2002. Lipid biomarkers indicate different ecological niches and trophic relationships of the Arctic hyperiid amphipods *Themisto abyssorum* and *T. libellula*. *Polar Biol.* 25, 374–383. <https://doi.org/10.1007/s00300-001-0354-7>.

- Auel, H., Klages, M., Werner, I., 2003. Respiration and lipid content of the Arctic copepod *Calanus hyperboreus* overwintering 1 m above the seafloor at 2,300 m water depth in the Fram Strait. *Mar. Biol.* 143, 275–282. <https://doi.org/10.1007/s00227-003-1061-4>.
- Barber, D.G., Hop, H., Mundy, C.J., Else, B., Dmitrenko, I.A., Tremblay, J.E., Ehn, J.K., Assmy, P., Daase, M., Candlish, L.M., Rysgaard, S., 2015. Selected physical, biological and biogeochemical implications of a rapidly changing Arctic Marginal Ice Zone. *Prog. Oceanogr.* 139, 122–150. <https://doi.org/10.1016/j.pocean.2015.09.003>.
- Basedow, S.L., Sundfjord, A., von Appen, W.J., Halvorsen, E., Kwasniewski, S., Reigstad, M., 2018. Seasonal variation in transport of zooplankton into the Arctic basin through the Atlantic gateway, Fram Strait. *Front. Mar. Sci.* 5, 1–22. <https://doi.org/10.3389/fmars.2018.00194>.
- Berge, J., Daase, M., Renaud, P.E., Ambrose, W.G., Darnis, G., Last, K.S., Leu, E., Cohen, J.H., Johnsen, G., Moline, J.A., Cottier, F., Varpe, O., Shunatova, N., Balazy, P., Morata, N., Massabuau, J.C., Falk-Petersen, S., Kosobokova, K., Hoppe, C. J., Weślawski, J.M., Kuklinski, P., Legeżyńska, J., Nikishina, D., Cusa, M., Kędra, M., Włodarska-Kowalczyk, M., Vogedes, D., Camus, L., Tran, D., Michaud, E., Gabrielsen, T.M., Granovitch, A., Gonchar, A., Krapp, R., Callesen, T.A., 2015. Unexpected levels of biological activity during the polar night offer new perspectives on a warming arctic. *Curr. Biol.* 25, 2555–2561. <https://doi.org/10.1016/j.cub.2015.08.024>.
- Brandt, S., Wassmann, P.F.J., Piepenburg, D., 2023. Revisiting the footprints of climate change in Arctic marine food webs: An assessment of knowledge gained since 2010. *Front. Mar. Sci.* 10, 65. <https://doi.org/10.3389/fmars.2023.1096222>.
- Cabrol, J., Trombetta, T., Amaudrut, S., Aulanier, F., Sage, R., Tremblay, R., Nozais, C., Starr, M., Plourde, S., Winkler, G., 2019. Trophic niche partitioning of dominant North-Atlantic krill species, *Meganyctiphanes norvegica*, *Thysanoessa inermis*, and *T. raschii*. *Limnol. Oceanogr.* 64, 165–181. <https://doi.org/10.1002/lno.11027>.
- Carmack, E., McLaughlin, F., 2011. Towards recognition of physical and geochemical change in Subarctic and Arctic seas. *Prog. Oceanogr.* 90, 90–104. <https://doi.org/10.1016/j.pocean.2011.02.007>.
- Cavaliere, D.J., Parkinson, C.L., Gloersen, P., Zwally, H.J., 1996. Sea ice concentrations from nimbus-7 SMMR and DMSP SSM/I-SSMIS passive microwave data, version 1, updated yearly. NASA National Snow and Ice Data Center Distributed Active Archive Center. Boulder, Colorado USA [Accessed 27.01.2022] doi:10.5067/8GQ8LZQVLOVL.
- Choquet, M., Kosobokova, K., Kwasniewski, S., Hatlebakk, M., Dhanasiri, A.K., Melle, W., Daase, M., Svensen, C., Søreide, J.E., Hoarau, G., 2018. Can morphology reliably distinguish between the copepods *Calanus finmarchicus* and *C. glacialis*, or is DNA the only way? *Limnol. Oceanogr. Methods* 16, 237–252. <https://doi.org/10.1002/lom3.10240>.
- Crews, L., Sundfjord, A., Hattermann, T., 2019. How the Yermak Pass Branch regulates Atlantic Water inflow to the Arctic Ocean. *J. Geophys. Res. Oceans* 124, 267–280. <https://doi.org/10.1029/2018JC014476>.
- Dale, K., Falk-Petersen, S., Hop, H., Fevolden, S.E., 2006. Population dynamics and body composition of the Arctic hyperiid amphipod *Themisto libellula* in Svalbard fjords. *Polar Biol.* 29, 1063–1070. <https://doi.org/10.1007/s00300-006-0150-5>.
- Dalpadado, P., 2002. Inter-specific variations in distribution, abundance and possible life-cycle patterns of *Themisto* spp. (Amphipoda) in the Barents Sea. *Polar Biol.* 25, 656–666. <https://doi.org/10.1007/s00300-002-0390-y>.
- Dalpadado, P., Ellertsen, B., Johannessen, S., 2008a. Inter-specific variations in distribution, abundance and reproduction strategies of krill and amphipods in the Marginal Ice Zone of the Barents Sea. *Deep-Sea Res. Part II: Topical Stud. Oceanogr.* 55, 2257–2265. <https://doi.org/10.1016/j.dsr2.2008.05.015>.
- Dalpadado, P., Arrigo, K.R., van Dijken, G.L., Skjoldal, H.R., Bagoien, E., Dolgov, A.V., Prokophchuk, I.P., Sperfeld, E., 2020. Climate effects on temporal and spatial dynamics of phytoplankton and zooplankton in the Barents Sea. *Prog. Oceanogr.* 185, 102320 <https://doi.org/10.1016/j.pocean.2020.102320>.
- Dalpadado, P., Ingvaldsen, R.B., Stige, L.C., Bogstad, B., Knut sen, T., Ottersen, G., Ellertsen, B., 2012. Climate effects on Barents Sea ecosystem dynamics. *ICES J. Mar. Sci.* 69, 1303–1316. doi:10.1093/icesjms/fgs063.
- Dalpadado, P., Arrigo, K.R., Hjøllø, S.S., Rey, F., Ingvaldsen, R.B., Sperfeld, E., Van Dijken, G.L., Stige, L.C., Olsen, A., Ottersen, G., 2014. Productivity in the Barents Sea - Response to recent climate variability. *PLoS ONE* 9. doi:10.1371/journal.pone.0095273.
- Dalpadado, P., Hop, H., Rønning, J., Pavlov, V., Sperfeld, E., Buchholz, F., Rey, A., Wold, A., 2016. Distribution and abundance of euphausiids and pelagic amphipods in Kongsfjorden and Rijpfjorden (Svalbard) and changes in their relative importance as key prey in a warming marine ecosystem. *Polar Biol.* 39, 1765–1784. doi:10.1007/s00300-015-1874-x.
- Dalpadado, P., Mowbray, F., 2013. Comparative analysis of feeding ecology of capelin from two shelf ecosystems, off Newfoundland and in the Barents Sea. *Prog. Oceanogr.* 114, 97–105. <https://doi.org/10.1016/j.pocean.2013.05.007>.
- Dalpadado, P., Skjoldal, H.R., 1996. Abundance, maturity and growth of the krill species *Thysanoessa inermis* and *T. longicaudata* in the Barents Sea. *Mar. Ecol. Prog. Ser.* 144, 175–183. <https://doi.org/10.3354/meps144175>.
- Dalpadado, P., Yamaguchi, A., Ellertsen, B., Johannessen, S., 2008b. Trophic interactions of macro-zooplankton (krill and amphipods) in the Marginal Ice Zone of the Barents Sea. *Deep Sea Res. Part II* 55, 2266–2274. <https://doi.org/10.1016/j.dsr2.2008.05.016>.
- David, C., Lange, B., Rabe, B., Flores, H., 2015. Community structure of under-ice fauna in the Eurasian central Arctic Ocean in relation to environmental properties of sea ice habitats. *Mar. Ecol. Prog. Ser.* 522, 15–32. <https://doi.org/10.3354/meps11556>.

- de Santana, C.N., Rozenfeld, A.F., Marquet, P.A., Duarte, C.M., 2013. Topological properties of polar food webs. *Mar. Ecol. Prog. Ser.* 474, 15–26. <https://doi.org/10.3354/meps10073>.
- Dolgov, A., Orlova, E., Johannessen, E., Bogstad, B., Rudneva, G., Dalpadado, P., Mukhina, N., 2011. Planktivorous fishes. In: Jakobsen, T., Ozhigin, V. (Eds.), *The Barents Sea. Ecosystem, Resources, Management. Half a Century of Russian-Norwegian Cooperation*. Tapir Press, Trondheim, Norway, pp. 438–454.
- Ehrlich, J., Schaafsma, F. L., Bluhm, B. A., Peeken, I., Castellani, G., Brandt, A., Flores, H., 2020. Sympagic Fauna in and under Arctic pack ice in the annual sea-ice system of the new Arctic. *Front. Mar. Sci.*, 7(June). doi:10.3389/fmars.2020.00452.
- Ershova, E.A., Kosobokova, K.N., Banas, N.S., Ellingsen, I., Nieho, B., Hildebrandt, N., Hirche, H.J., 2021. Sea ice decline drives biogeographical shifts of key *Calanus* species in the central Arctic Ocean. *Glob. Chang. Biol.* 27, 2128–2143. <https://doi.org/10.1111/gcb.15562>.
- Falk-Petersen, S., Mayzaud, P., Kattner, G., Sargent, J.R., 2009. Lipids and life strategy of Arctic *Calanus*. *Mar. Biol. Res.* 5, 18–39. <https://doi.org/10.1080/17451000802512267>.
- Flores, H., David, C., Ehrlich, J., Hardge, K., Kohlbach, D., Lange, B.A., Niehoff, B., Nöthig, E.M., Peeken, I., Metfies, K., 2019. Sea-ice properties and nutrient concentration as drivers of the taxonomic and trophic structure of high-Arctic protist and metazoan communities. *Polar Biol.* 42 (7), 1377–1395. <https://doi.org/10.1007/s00300-019-02526-z>.
- Geoffroy, M., Daase, M., Cusa, M., Darnis, G., Graeve, M., Santana Hernández, N., Berge, J., Renaud, P.E., Cottier, F., Falk-Petersen, S., 2019. Mesopelagic sound scattering layers of the High Arctic: Seasonal variations in biomass, species assemblage, and trophic relationships. *Front. Mar. Sci.* 6 <https://doi.org/10.3389/fmars.2019.00364>.
- Gluchowska, M., Dalpadado, P., Beszczynska-Möller, A., Ol szewska, A., Ingvaldsen, R.B., Kwasiński, S., 2017. Inter-annual zooplankton variability in the main pathways of the Atlantic water flow into the Arctic Ocean (Fram Strait and Barents Sea branches). *ICES J. Mar. Sci.* 74, 1921–1936. doi:10.1093/icesjms/fsx033.
- Good, S., Fiedler, E., Mao, C., Martin, M.J., Maycock, A., Reid, R., Roberts-Jones, J., Searle, T., Waters, J., While, J., Worsfold, M., 2020. The current configuration of the Ostia system for operational production of foundation sea surface temperature and ice concentration analyses. *Remote Sens. (Basel)* 12. <https://doi.org/10.3390/rs12040720>.
- Gradinger, R., Bluhm, B.A., Hopcroft, R.R., Gebruk, A.V., Kosobokova, K., Sirenko, B., Węślawski, J.M., 2010. *Marine Life in the Arctic*. John Wiley & Sons, Ltd, Oxford, United Kingdom. chapter 10. pp. 183–202. <https://doi.org/10.1002/9781444325508.ch10>.
- Greenacre, M., 1983. *Theory and applications of Correspondence Analysis*. Academic Press.
- Greenacre, M., 2017. *Correspondence Analysis in practice*, 3rd ed., CRC Press.
- Greenacre, M., Primmer, R., 2013. *Multivariate Analysis of Ecological Data*. Fundación BBVA.
- Grigor, J.J., Schmid, M.S., Caouette, M., St-Onge, V., Brown, T.A., Barthélémy, R.M., 2020. Non-carnivorous feeding in Arctic chaetognaths. *Progress Oceanogr.* 186, 102388. URL: <https://doi.org/10.1016/j.pocean.2020.102388>.
- Grigor, J.J., Søreide, J.E., Varpe, Ø., 2014. Seasonal ecology and life-history strategy of the high-latitude predatory zooplankton *Parasagitta elegans*. *Mar. Ecol. Prog. Ser.* 499, 77–88. <https://doi.org/10.3354/meps10676>.
- Grigor, J.J., Schmid, M.S., Fortier, L., 2017. Growth and reproduction of the chaetognaths *Eukrohnia hamata* and *Parasagitta elegans* in the Canadian arctic ocean: capital breeding versus income breeding. *J. Plankton Res.* 39, 910–929. <https://doi.org/10.1093/plankt/fbx045>.
- Havermans, C., Auel, H., Hagen, W., Held, C., Ensor, N.S., Tarling, G.A., 2019. Predatory zooplankton on the move: *Themisto* amphipods in high-latitude marine pelagic food webs. In: *Advances in marine biology*, Vol. 82. Academic Press, pp. 51–92.
- Hobbs, L., Banas, N.S., Cottier, F.R., Berge, J., Daase, M., 2020. Eat or Sleep: Availability of winter prey explains mid-winter and spring activity in an Arctic *Calanus* population. *Front. Mar. Sci.* 7, 1–14. <https://doi.org/10.3389/fmars.2020.541564>.
- Hop, H., Wold, A., Meyer, A., Bailey, A., Hatlebakk, M., Kwasiński, S., Leopold, P., Kuklinski, P., Søreide, J.E., 2021. Winter-spring development of the zooplankton community below sea ice in the Arctic Ocean. *Front. Mar. Sci.* 8 <https://doi.org/10.3389/fmars.2021.609480>.
- Hunt, B.P., Pakhomov, E.A., Siegel, V., Strass, V., Cisewski, B., Bathmann, U., 2011. The seasonal cycle of the Lazarev Sea macrozooplankton community and a potential shift to top down trophic control in winter. *Deep-Sea Res. Part II: Topical Stud. Oceanogr.* 58, 1662–1676. doi:10.1016/j.jdsr.2.2010.11.016.
- ICES, 2020. The Working Group on the Integrated Assessments of the Barents Sea (WGIBAR). *ICES Sci. Reports* 2, 157. <https://doi.org/10.17895/ices.pub.5998>.
- ICES, 2021. The Working Group on the Integrated Assessments of the Barents Sea (WGIBAR). *ICES Sci. Reports* 3, 236. <https://doi.org/10.17895/ices.pub.8241>.
- ICES, 2017. Manual for the Midwater Ring Net sampling during IBTS Q1. Series of ICES Survey Protocols SISP 2. *ICES Scientific Reports* , 25, doi:10.17895/ices.pub.3434.
- Ikeda, T., Skjoldal, H.R., 1989. Metabolism and elemental composition of zooplankton from the Barents Sea during early Arctic summer. *Mar. Biol.* 100, 173–183. <https://doi.org/10.1007/BF00391956>.
- Ingvaldsen, R.B., Assmann, K.M., Primmer, R., Fossheim, M., Polyakov, I.V., Dolgov, A. V., 2021. Physical manifestations and ecological implications of Arctic Atlantification. *Nature Rev. Earth Environ.* 2, 874–889. <https://doi.org/10.1038/s43017-021-00228-x>.
- Ingvaldsen, R.B., Eriksen, E., Gjøseter, H., Engås, A., Schuppe, B.K., Assmann, K.M., Cannaby, H., Dalpadado, P., Bluhm, B.A., 2023. Under-ice observations by trawls and multi-frequency acoustics in the Central Arctic Ocean reveals abundance and composition of pelagic fauna. *Sci. Rep.* 13, 1000. <https://doi.org/10.1038/s41598-023-27957-x>.
- Ivanov, V.V., Polyakov, I.V., Dmitrenko, I.A., Hansen, E., Repina, I.A., Kirillov, S.A., Mauritzen, C., Simmons, H., Timokhov, L.A., 2009. Seasonal variability in Atlantic Water off Spitsbergen. *Deep Sea Res. Part 1 Oceanogr. Res. Pap.* 56, 1–14. <https://doi.org/10.1016/j.dsr.2008.07.013>.
- Kaartvedt, S., Titelman, J., 2018. Planktivorous fish in a future Arctic Ocean of changing ice and unchanged photoperiod. *ICES J. Mar. Sci.* 75, 2312–2318. doi:10.1093/icesjms/fsx248.
- Kaartvedt, S., Larsen, T., Hjelmseth, K., Onsrud, M.S., 2002. Is the omnivorous krill *Meganyctiphanes norvegica* primarily a selectively feeding carnivore? *Mar. Ecol. Prog. Ser.* 228, 193–204. <https://doi.org/10.3354/meps228193>.
- Kaiser, P., Hagen, W., Bode-Dalby, M., Auel, H., 2022. Tolerant but facing increased competition: Arctic zooplankton versus Atlantic invaders in a warming ocean. *Front. Mar. Sci.* 9, 908638. <https://doi.org/10.3389/fmars.2022.908638>.
- Knutsen, T., Wiebe, P.H., Gjøseter, H., Ingvaldsen, R.B., Lien, G., 2017. High Latitude Epipelagic and Mesopelagic Scattering Layers - a reference for future Arctic ecosystem change. *Front. Mar. Sci.* 4 <https://doi.org/10.3389/fmars.2017.00334>.
- Kohlbach, D., Schmidt, K., Hop, H., Wold, A., Al-Hababeh, A.K., Belt, S.T., Woll, M., Graeve, M., Smik, L., Atkinson, A., Assmy, P., 2021. Winter carnivory and diapause counteract the reliance on ice algae by Barents Sea zooplankton. *Front. Mar. Sci.* 8: 640050. doi:10.3389/fmars.2021.640050.
- Kohlbach, D., Schaafsma, F.L., Graeve, M., Lebreton, B., Lange, B.A., David, C., Vortkamp, M., Flores, H., 2017. Strong linkage of polar cod (*Boreogadus saida*) to sea ice algae-produced carbon: Evidence from stomach content, fatty acid and stable isotope analyses. *Prog. Oceanogr.* 152, 62–74. <https://doi.org/10.1016/j.pocean.2017.02.003>.
- Kortsch, S., Primmer, R., Fossheim, M., Dolgov, A.V., Aschan, M., 2015. Climate change alters the structure of arctic marine food webs due to poleward shifts of boreal generalists. *Proc. Roy. Soc. B: Biol. Sci.* 282. doi:10.1098/rspb.2015.1546.
- Kortsch, S., Primmer, R., Aschan, M., Lind, S., Dolgov, A.V., Planque, B., 2019. Food-web structure varies along environmental gradients in a high-latitude marine ecosystem. *Ecography* 42, 295–308. <https://doi.org/10.1111/ecog.03443>.
- Kosobokova, K., Hirche, H.J., 2009. Biomass of zooplankton in the eastern Arctic Ocean - A base line study. *Prog. Oceanogr.* 82, 265–280. <https://doi.org/10.1016/j.pocean.2009.07.006>.
- Kosobokova, K.N., Hopcroft, R.R., Hirche, H.J., 2011. Patterns of zooplankton diversity through the depths of the Arctic's central basins. *Mar. Biodivers.* 41 (1), 29–50. <https://doi.org/10.1007/s12526-010-0057-9>.
- Koszteyn, J., Timofeev, S., Węślawski, J.M., Malinga, B., 1995. Size structure of *Themisto abyssorum* (Boeck) and *Themisto libellula* (Mandt) populations in European Arctic seas. *Polar Biol.* 15, 85–92. <https://doi.org/10.1007/BF00241046>.
- Kraft, A., Nöthig, E.M., Bauerfeind, E., Wildish, D.J., Pohle, G.W., Bathmann, U.V., Beszczynska-Möller, A., Klages, M., 2013. First evidence of reproductive success in a southern invader indicates possible community shifts among Arctic zooplankton. *Mar. Ecol. Prog. Ser.* 493, 291–296.
- Kunisch, E.H., Bluhm, B.A., Daase, M., Gradinger, R., Hop, H., Melnikov, I.A., Varpe, Ø., Berge, J., 2020. Pelagic occurrences of the ice amphipod *Apherusa glacialis* throughout the Arctic. *J. Plankton Res.* 42, 73–86. <https://doi.org/10.1093/plankt/fbz072>.
- Landrum, L., Holland, M.M., 2020. Extremes become routine in an emerging new Arctic. *Nat. Clim. Chang.* 10, 1108–1115. <https://doi.org/10.1038/s41558-020-0892-z>.
- Langbehn, T.J., Varpe, Ø., 2017. Sea-ice loss boosts visual search: fish foraging and changing pelagic interactions in polar oceans. *Global Change Biol.* 23, 5318–5330. doi:10.1111/gcb.13797.
- Legendre, P., Legendre, L., 2012. *Numerical Ecology*, 3rd ed., Elsevier.
- Lewis, K.M., Van Dijken, G.L., Arrigo, K.R., 2020. Changes in phytoplankton concentration now drive increased Arctic Ocean primary production. *Science* 369, 198–202. doi:10.1126/science.aay8380.
- Lind, S., Ingvaldsen, R.B., Furevik, T., 2018. Arctic warming hotspot in the northern Barents Sea linked to declining sea ice import. *Nature Climate Change* 8, 634–639. doi:10.1038/s41558-018-0205-y.
- Lind, S., Ingvaldsen, R.B., 2012. Variability and impacts of Atlantic Water entering the Barents Sea from the north. *Deep Sea Res. Part I* 62, 70–88. <https://doi.org/10.1016/j.dsr.2011.12.007>.
- Loeng, H., 1991. Features of the physical oceanographic conditions of the Barents Sea. *Polar Res.* 10, 5 18. doi:10.1111/j.1751-8369.1991.tb00630.x.
- Lundesgaard, O., Sundfjord, A., Lind, S., Nilsen, F., Renner, A.H.H., 2022. Import of Atlantic water and sea ice control the ocean environment in the northern Barents Sea. *Ocean Science Discussions [Preprint]* 2022, 1–43. URL: <https://os.copernicus.org/preprints/os-2022-17/>, doi:10.5194/os-2022-17.
- Macnaughton, M.O., Thormar, J., Berge, J., 2007. Sympagic amphipods in the Arctic pack ice: Redescriptions of *Eusirus holmii* Hansen, 1887 and *Pleusymtes karstensi* (Barnard, 1959). *Polar Biol.* 30, 1013–1025. doi:10.1007/s00300-007-0260-8.
- Maňko, M.K., Gluchowska, M., Weydmann-Zwoliczka, A., 2020. Footprints of Atlantification in the vertical distribution and diversity of gelatinous zooplankton in the Fram Strait (Arctic Ocean). *Progress in Oceanography* 189, 102414. doi:10.1016/j.pocean.2020.102414.
- Michalsen, K., Dalpadado, P., Eriksen, E., Gjøseter, H., Ingvaldsen, R.B., Johannessen, E., Jørgensen, L.L., Knutsen, T., Prozorkevich, D., Skern-Mauritzen, M., 2013. Marine living resources of the Barents Sea - Ecosystem understanding and monitoring in a climate change perspective. *Mar. Biol. Res.* 9, 932–947. <https://doi.org/10.1080/17451000.2013.775459>.
- Mumm, N., Auel, H., Hanssen, H., Hagen, W., Richter, C., Hirche, H.-J., 1998. Breaking the ice: large-scale distribution of mesozooplankton after a decade of Arctic and transpolar cruises. *Polar Biol.* 20, 189–197.

- Nansen, F., 1901. *The Norwegian North Polar Expedition, 1893–1896: Scientific Results, volume 2. Longmans, Green and Company.*
- Noyon, M., Narcy, F., Gasparini, S., Mayzaud, P., 2011. Growth and lipid class composition of the Arctic pelagic amphipod *Themisto libellula*. *Mar. Biol.* 158, 883–892. doi:10.1007/s00227-010-1615-1.
- Oksanen, J., Blanchet, F.G., Friendly, M., Kindt, R., Legendre, P., McGinn, D., Minchin, P.R., O'Hara, R.B., Simpson, G.L., Solymos, P., Stevens, M.H.H., Szoecs, E., Wagner, H., 2019. *vegan: Community Ecology Package*. URL: <https://CRAN.R-project.org/package=vegan>. r package version 2.5-6.
- Onarheim, I.H., Eldevik, T., Smedsrud, L.H., Stroeve, J.C., 2018. Seasonal and regional manifestation of Arctic sea ice loss. *J. Climate* 31, 4917–4932. doi:10.1175/JCLI-D-17-0427.1.
- Orlova, E.L., Dolgov, A.V., Renaud, P.E., Boitsov, V.D., Prokopchuk, I.P., Zashihina, M.V., 2013. Structure of the macroplankton-pelagic fish-cod trophic complex in a warmer Barents Sea. *Mar. Biol. Res.* 9, 851–866. <https://doi.org/10.1080/17451000.2013.775453>.
- Orlova, E.L., Dolgov, A.V., Renaud, P.E., Greenacre, M., Halsband, C., Ivshin, V.A., 2015. Climatic and ecological drivers of euphausiid community structure vary spatially in the Barents Sea: Relationships from a long time series (1952–2009). *Front. Mar. Sci.* 1, 1–13. <https://doi.org/10.3389/fmars.2014.00074>.
- Percy, J.A., 1993. Energy consumption and metabolism during starvation in the Arctic hyperiid amphipod *Themisto libellula* Mandt. *Polar Biol.* 13, 549–555. <https://doi.org/10.1007/BF00236397>.
- Percy, J., Fife, F., 1981. The Biochemical Composition and Energy Content of Arctic Marine Macrozooplankton. *Arctic* 34, 307–313. <https://doi.org/10.14430/arctic2533>.
- Pinheiro, J., Bates, D., DebRoy, S., Sarkar, D., R Core Team, 2020. *nlme: Linear and Nonlinear Mixed Effects Models*. URL: <https://CRAN.R-project.org/package=nlme>. r package version 3.1-148.
- Planque, B., Primicerio, R., Michalsen, K., Aschan, M., Certain, G., Dalpadado, P., Gjørseter, H., Hansen, C., Johannesen, E., Jørgensen, L.L., Kolsum, I., Kortsch, S., Leclerc, L.M., Omli, L., Skern-Mauritzen, M., Wiedmann, M., 2014. Who eats whom in the Barents Sea: a food web topology from plankton to whales. *Ecology* 95, 1430–1430. doi:10.1890/13-1062.1.
- R Core Team, 2020. *R: A Language and Environment for Statistical Computing*. R Foundation for Statistical Computing, Vienna, Austria. URL: <https://www.R-project.org/>.
- Renaud, P.E., Daase, M., Banas, N.S., Gabrielsen, T.M., Søreide, J.E., Varpe, O., Cottier, F., Falk-Petersen, S., Halsband, C., Vogedes, D., Heggland, K., Berge, J., Andersen, K., 2018. Pelagic food-webs in a changing Arctic: a trait-based perspective suggests a mode of resilience. *ICES J. Mar. Sci.* 75, 1871–1881. <https://doi.org/10.1093/icesjms/fsy063>.
- Renner, A.H., Sundfjord, A., Janout, M.A., Ingvaldsen, R.B., Beszczynska-Möller, A., Pickart, R.S., Pérez-Hernández, M.D., 2018. Variability and redistribution of heat in the Atlantic Water Boundary Current north of Svalbard. *J. Geophys. Res.: Oceans* 123, 6373–6391. doi:10.1029/2018JC013814.
- Ressler, P.H., Dalpadado, P., Macaulay, G.J., Handegard, N., Skern-Mauritzen, M., 2015. Acoustic surveys of euphausiids and models of baleen whale distribution in the Barents Sea. *Mar. Ecol. Progress Series* 527, 13–29. doi:10.3354/meps11257.
- Rudels, B., Korhonen, M., Schauer, U., Pisarev, S., Rabe, B., Wisotzki, A., 2015. Circulation and transformation of Atlantic water in the Eurasian Basin and the contribution of the Fram Strait in ow branch to the Arctic Ocean heat budget. *Prog. Oceanogr.* 132, 128–152. <https://doi.org/10.1016/j.pocean.2014.04.003>.
- Scott, C.L., Kwasniewski, S., Falk-Petersen, S., Sargent, J.R., 2000. Lipids and life strategies of *Calanus finmarchicus*, *Calanus glacialis* and *Calanus hyperboreus* in late autumn, Kongsfjorden, Svalbard. *Polar Biology* 23, 510–516. doi:10.1007/s003000000114.
- Sivel, E., Planque, B., Lindstrøm, U., Yoccoz, N.G., 2021. Multiple configurations and fluctuating trophic control in the Barents Sea food-web. *PLoS ONE* 16 (7), e0254015. <https://doi.org/10.1371/journal.pone.0254015>.
- Søreide, J.E., Leu, E.V., Berge, J., Graeve, M., Falk-Petersen, S., 2010. Timing of blooms, algal food quality and *Calanus glacialis* reproduction and growth in a changing Arctic. *Glob. Chang. Biol.* 16, 3154–3163. <https://doi.org/10.1111/j.1365-2486.2010.02175.x>.
- Stige, L.C., Eriksen, E., Dalpadado, P., Ono, K., 2019a. Direct and indirect effects of sea ice cover on major zooplankton groups and planktivorous fishes in the Barents Sea. *ICES J. Mar. Sci.* 76, 124–136. <https://doi.org/10.1093/icesjms/fsz063>.
- Stige, L.C., Rogers, L.A., Neuheimer, A.B., Hunsicker, M.E., Yarovina, N.A., Ottersen, G., Ciannelli, L., Langangen, Ø., Durant, J.M., 2019b. Density- and size-dependent mortality in early life stages. *Fish Fish.* 20, 962–976. <https://doi.org/10.1111/faf.12391>.
- Stroeve, J., Notz, D., 2018. Changing state of Arctic sea ice across all seasons. *Environ. Res. Lett.* 13 <https://doi.org/10.1088/1748-9326/aade56>.
- Sundfjord, A., Assmann, K.M., Lundesgaard, Ø., Renner, A.H.H., Lind, S., Ingvaldsen, R. B., 2020. Suggested water mass definitions for the central and northern Barents Sea, and the adjacent Nansen Basin. The Nansen Legacy Report Series. <https://doi.org/10.7557/nlrs.5707>.
- ter Braak, C.J., Verdonschot, P.F., 1995. Canonical correspondence analysis and related multivariate methods in aquatic ecology. *Aquatic Sci.* 57, 255–289. doi:10.1007/BF00877430.
- Vader, A., 2022. Chlorophyll a and phaeopigments Nansen Legacy. doi:10.21335/NMDC-1371694848.
- Vinogradov, G.M., 1999. Deep-sea near-bottom swarms of pelagic amphipods *Themisto*: Observations from submersibles. *Sarsia* 84, 465–467. <https://doi.org/10.1080/00364827.1999.10807352>.
- Wassmann, P., Carmack, E.C., Bluhm, B.A., Duarte, C.M., Berge, J., Brown, K., Grebmeier, J.M., Holding, J., Kosobokova, K., Kwok, R., Matrai, P., Agustí, S., Babin, M., Bhatt, U., Eicken, H., Polyakov, I., Rysgaard, S., Huntington, H.P., 2020. Towards a unifying pan-Arctic perspective: A conceptual modelling toolkit. *Prog. Oceanogr.* 189, 102455 <https://doi.org/10.1016/j.pocean.2020.102455>.
- Wassmann, P., Duarte, C.M., Agustí, S., Sejr, M.K., 2011. Footprints of climate change in the Arctic marine ecosystem. *Global Change Biol.* 17, 1235–1249. doi:10.1111/j.1365-2486.2010.02311.x.
- Wold, A., Hop, H., Svendsen, Assmann, K., Kwasniewski, S., Ormacyk, M., Søreide, C., 2023. Atlantification influences zooplankton communities seasonally in the northern Barents Sea and Arctic Ocean. *Progress in Oceanography*, this issue.
- Zhukova, N.G., Nesterova, V.N., Prokopchuk, I.P., Rudneva, G.B., 2009. Winter distribution of euphausiids (Euphausiacea) in the Barents Sea (2000–2005) 56, 1959–1967. doi:10.1016/j.dsr2.2008.11.007.